iScience

CellPress
OPEN ACCESS

Article

Plasma endocannabinoidome and fecal microbiota interplay in people with HIV and subclinical coronary artery disease: Results from the Canadian HIV and Aging Cohort Study

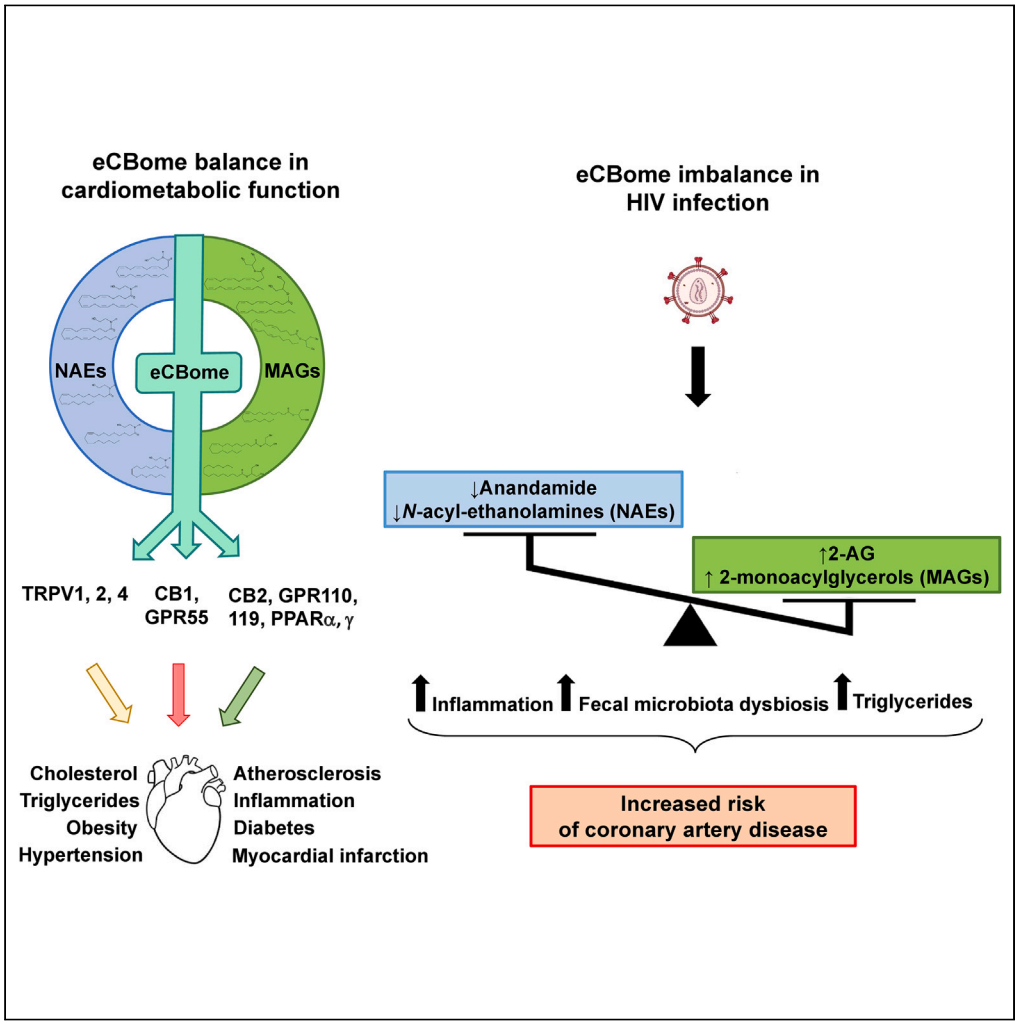

Ralph-Sydney Mboumba Bouassa, Giada Giorgini, Cristoforo Silvestri, ..., Cecilia T. Costiniuk, Vincenzo Di Marzo, Mohammad-Ali Jenabian

jenabian.mohammad-ali@uqam.ca (M.-A.J.)
vincenzo.di-marzo.1@ulaval.ca (V.D.)

Highlights

HIV infection is associated with perturbed plasma endocannabinoidome mediators

Plasma triglycerides are associated with enhanced 2-monoacylglycerol (MAG) levels

N-acyl-ethanolamine and MAG inverse relation may predict subclinical CAD in PWH

CAD-associated taxonomic alterations in fecal bacterial taxa were not found in PWH

Mboumba Bouassa et al., iScience 27, 110456
August 16, 2024
https://doi.org/10.1016/j.isci.2024.110456

iScience

CellPress
OPEN ACCESS

Article

Plasma endocannabinoidome and fecal microbiota interplay in people with HIV and subclinical coronary artery disease: Results from the Canadian HIV and Aging Cohort Study

Ralph-Sydney Mboumba Bouassa,[1,2,9] Giada Giorgini,[3,9] Cristoforo Silvestri,[3,4] Chanté Muller,[3] Nayudu Nallabelli,[3] Yulia Alexandrova,[1] Madeleine Durand,[5] Cécile Tremblay,[5] Mohamed El-Far,[5] Carl Chartrand-Lefebvre,[5] Marc Messier-Peet,[5] Shari Margolese,[6] Nicolas Flamand,[3] Cecilia T. Costiniuk,[2,7] Vincenzo Di Marzo,[3,4,8,10,*] and Mohammad-Ali Jenabian[1,10,11,*]

SUMMARY

Chronic HIV infection is associated with accelerated coronary artery disease (CAD) due to chronic inflammation. The expanded endocannabinoid system (eCBome) and gut microbiota modulate each other and are key regulators of cardiovascular functions and inflammation. We herein investigated the interplay between plasma eCBome mediators and gut microbiota in people with HIV (PWH) and/or subclinical CAD versus HIV-uninfected individuals. CAD was determined by coronary computed tomography (CT) angiography performed on all participants. Plasma eCBome mediator and fecal microbiota composition were assessed by tandem mass spectrometry and 16S rDNA sequencing, respectively. HIV infection was associated with perturbed plasma eCBome mediators characterized by an inverse relationship between anandamide and *N*-acyl-ethanolamines (NAEs) versus 2-AG and 2-monoacylglycerols (MAGs). Plasma triglyceride levels were positively associated with MAGs. Several fecal bacterial taxa were altered in HIV−CAD+ versus controls and correlated with plasma eCBome mediators. CAD-associated taxonomic alterations in fecal bacterial taxa were not found in PWH.

INTRODUCTION

Despite the success of antiretroviral therapy (ART) to suppress HIV viral replication, people with HIV (PWH) suffer from premature age-related comorbidities, due to a persistent and chronic inflammatory status known as "inflamm-aging." This results in accelerated comorbidities, notably atherosclerosis and coronary artery disease (CAD), which are the leading causes of non-acquired immunodeficiency syndrome (AIDS)-related morbidity and mortality.[1–5] It is estimated that by 2030, at least 78% of PWH will have subclinical or clinical CAD, which is now a major cause of death in this population.[6,7] Besides traditional cardiovascular risk factors (particularly tobacco smoking), and the relative toxicities associated with long-term exposure to ART, chronic inflammation and persistent immune activation associated with HIV are considered major contributors to the development of atherosclerotic plaques, a critical factor in the establishment of CAD.[6,7] Indeed, PWH typically exhibit systemic inflammation characterized by constant immune cell activation, resulting in persistent elevated levels of circulating pro-inflammatory and profibrotic cytokines such as interleukin (IL)-1β, IL-6, tumor necrosis factor alpha (TNF-α), interferon gamma (IFN-γ), soluble TNF receptor family (sTNFR), monocyte chemotactic factor (CCL2), soluble cluster of differentiation (sCD163 and sCD14), and intercellular adhesion molecule 1 (ICAM-1).[6] This chronic inflammatory state contributes to the dysfunction of vascular endothelial cells, abnormal lipid metabolism, hypercoagulation, inflammation, and fibrosis of vascular coronary tissues that promote the development of

[1]Department of Biological Sciences and CERMO-FC Research Centre, Université du Quebec à Montréal, Montreal, QC, Canada
[2]Infectious Diseases and Immunity in Global Health Program, Research Institute of the McGill University Health Centre, Montreal, QC, Canada
[3]Research Center of the Institut Universitaire de Cardiologie et Pneumologie de Québec (CRIUCPQ), Université Laval
[4]Institut sur la Nutrition et les Aliments Fonctionnels (INAF) et Centre Nutrition, Santé et Société (NUTRISS), Université Laval, Québec City, QC, Canada
[5]Centre de recherche du CHUM, Université de Montréal, Montreal, QC, Canada
[6]CIHR Canadian HIV Trials Network (CTN), Vancouver, BC, Canada
[7]Division of Infectious Diseases/Chronic Viral Illness Service, McGill University Health Centre, Royal Victoria Hospital, Montreal, QC, Canada
[8]Canada Excellence Research Chair on the Microbiome-Endocannabinoidome Axis in Metabolic Health, Université Laval
[9]These authors contributed equally
[10]These authors contributed equally
[11]Lead author
*Correspondence: jenabian.mohammad-ali@uqam.ca (M.-A.J.), vincenzo.di-marzo.1@ulaval.ca (V.D.)
https://doi.org/10.1016/j.isci.2024.110456

atheroma plaques and ultimately result in CAD.[6] Thus, reducing chronic inflammation could be a promising strategy for the management of CAD in PWH.[8]

Over the past few decades, the expanded endocannabinoid (eCB) system, also known as the "endocannabinoidome" (eCBome), has gained increasing interest, in particular because of its involvement in modulating several biological functions in the human body, including inflammation, lipid metabolism, and cardiovascular functions.[9–14] The eCB system includes the G-protein-coupled receptors (GPCRs), cannabinoid receptor type 1 (CB1R) and 2 (CB2R), and their endogenous ligands, the eCBs, anandamide (*N*-arachidonoylethanolamine; AEA), and 2-arachidonoylglycerol (2-AG). The eCBome also includes eCB-like lipid congeners from the *N*-acylethanolamine (NAE) and the monoacylglycerol (MAG) families and their GPCRs as well as other receptors, including the peroxisome-proliferator-activated nuclear receptor family and ligand-activated ion channels.[10,11,15] AEA and 2-AG and their respective congeners are primarily known to exert pro-homeostatic properties.[10–13,16–19] However, elevated circulating AEA and 2-AG levels have been associated with atherosclerosis in mouse models, where CB_1 activation was suggested to lead to activation of inflammatory myeloid cells[20–23] and to coronary vascular dysfunction in observational studies conducted in obese humans.[9,24–31] In contrast, other eCBome lipid members have been found to produce anti-atherosclerotic effects, often by functioning at non-CB_1 receptors and through anti-inflammatory mechanisms.[32] These observations suggest that perturbations in circulating levels of AEA and 2-AG, and by extension their structural congeners, may serve as biomarkers of cardiovascular disease.

Besides the eCBome, the gut microbiota plays a pivotal role in the context of cardiovascular diseases.[33–37,32,38] Indeed, gut microbiota alteration promotes increased production of generally pro- and anti-atherogenic metabolites such as trimethylamine (which is converted to trimethylamine *N*-oxide [TMAO] in the liver) and short-chain fatty acids (SCFAs), or secondary bile acids (BAs), respectively.[32,38] TMAO release into the systemic circulation has been linked to coronary plaques, peripheral artery disease, the severity of CAD, including stroke, myocardial infarction, and death.[39–41] While bacterially derived SCFAs may promote or attenuate high blood pressure depending on the GPCR pathway activated[32,38], they are generally considered to be beneficial in the context of cardiovascular health,[38,42] similar to secondary BAs.[43–45] However, given the variability within these classes of molecules and the fact that they are able to modulate several signaling pathways, their relationship with CAD is complex and requires further studies. On the other hand, eCBome mediators produce various effects on the composition of gut microbiota, as does the pharmacological and genetic manipulation of the eCBome.[46–51] As such, NAEs and 2-MAGs have been demonstrated to directly alter the gut microbiota composition both *in vitro* and *in vivo*.[46–51] In addition, pharmacological blockade of the CB_1 receptor in obese mice alters gut microbiota composition and attenuates inflammation.[49] Accordingly, desensitization of CB_1 in $Mgll^{-/-}$ mice, as a consequence of the overproduction of 2-AG, results in protection from diet-induced obesity in association with changes to the gut microbiome, including the inhibition of high-fat-diet-induced increases of *Lactobacillaceae*.[50]

HIV infection results in gut microbiota dysbiosis, which in turn drives immune activation and increased levels of pro-inflammatory cytokines.[52] Furthermore, a recent observational study has shown an altered eCBome profile along with elevated levels of inflammatory mediators, concomitant to reduced levels of AEA and some of its NAE congeners, whereas 2-AG levels were not affected by the HIV status, suggesting a differential impact of HIV on circulating eCBome mediator metabolism in PWH.[53] However, the interplay between gut microbiota and circulating eCBome lipids in PWH, notably in the context of subclinical CAD, remain to be uncovered.

Understanding the alterations of circulating eCBome lipids and of gut bacteria occurring in individuals with early clinical precursors of CAD may allow for the identification of a signature profile associated with premature forms of this condition in PWH. The present study aims to assess the association between changes in plasma levels of the eCBs AEA and 2-AG and their congeners as well as of gut microbiota composition with subclinical CAD in PWH.

RESULTS

Study participants

Characteristics of study participants are summarized in the Tables 1, S1, and S2. A total of 208 participants (175 males, 84.13%), median age (IQR) 56 years, were included in the study, including $n = 156$ PWH and $n = 52$ HIV− as control group. The median time from HIV diagnosis was 19 years (SEM) and median duration of ART was 15 years (SEM) (Table S2). The HIV+ group had more current tobacco smokers and cannabis smokers compared to HIV− (31% versus 13%, $p = 0.031$, and 26% versus 7.7%, $p = 0.006$, for tobacco and cannabis smoking, respectively). Most of the study participants were under statin treatment with equal proportions among HIV+ and HIV− groups. PWH had lower levels of total cholesterol (4.75 versus 5.07 mmol/L, $p = 0.039$), low-density lipoproteins (LDL) (2.61 versus 3.06 mmol/L, $p = 0.002$), and high-density lipoproteins (HDL) (1.18 versus 1.36 mmol/L, $p = 0.004$) compared to the HIV− controls, whereas HIV+ participants had higher levels of triglycerides (1.70 versus 1.35 mmol/L, $p = 0.050$) and insulin (76 versus 55 pmol/L, $p = 0.013$) as described in Table 1. Compared to CAD− participants, CAD+ individuals were more likely to have a family history of CAD (51% versus 41%, $p = 0.039$), being current tobacco smokers (36% versus 17%, $p = 0.001$), being on statin therapy (28% versus 14%, $p = 0.007$), with a higher Framingham score (10 versus 8, $p = 0.018$), and with higher triglycerides levels (1.81 versus 1.38 mmol/L, $p = 0.037$). Within CAD+ individuals, there were no significant difference in total plaque volume, volume of low attenuation plaque, and calcium score between PWH and HIV− participants (Table S1). Finally, within HIV+ participants, there were no significant difference in the duration of HIV diagnosis, ART initiation, and ART regimen between CAD+ and CAD− participants (Table S2).

Plasma levels of the endocannabinoids *N*-arachidonoylethanolamine and 2-arachidonoylglycerol and their congeners in study participants

Two main groups of eCBs and eCB-like lipids were assessed in all study participants. The first group corresponded to the *N*-acylethanolamines (NAE) group, which encompasses the eCB anandamide (*N*-arachidonoylethanolamine: AEA) and its congeners, including

Table 1. Characteristics of the study participants according to the HIV status and subclinical coronary artery disease

	HIV+ N = 156	HIV− N = 52	p value[a]	CAD+ N = 109	CAD− N = 99	p value[a]	HIV+CAD+ N = 87	HIV+CAD− N = 69	HIV−CAD+ N = 22	HIV−CAD− N = 30	p value[b]
Characteristics											
Sex [n (%)]			**<0.001**			0.4					**0.001**
Female	15 (9.6)	18 (35)		14 (14)	18 (18)		7 (8.0)	8 (12)	8 (36)	10 (33)	
Male	141 (90)	34 (65)		94 (86)	81 (82)		80 (92)	61 (88)	14 (64)	20 (67)	
Age at study visit (years) [Median (IQR)]	56 (52–62)	58 (52–64)	0.2	59 (53–63)	55 (50–60)	**<0.001**	57 (52–62)	55 (51–60)	63 (59–69)	55 (50–58)	**<0.001**
HIV status [n (%)]			NA			0.11					NA
HIV−	NA	NA		22 (20)	30 (30)		NA	NA	NA	NA	
HIV+	NA	NA		87 (80)	69 (70)		NA	NA	NA	NA	
CAD status [n (%)]			0.11			NA					NA
CAD−	69 (44)	30 (58)		NA	NA		NA	NA	NA	NA	
CAD+	87 (56)	22 (42)		NA	NA		NA	NA	NA	NA	
CMV-IgG status [n (%)]			**<0.001**			0.6					**<0.001**
Negative	16 (10)	25 (48)		19 (17)	22 (22)		8 (9.2)	8 (12)	11 (50)	14 (47)	
Positive	124 (79)	19 (37)		78 (72)	65 (66)		69 (79)	55 (80)	9 (41)	10 (33)	
Unknown	16 (10)	8 (15)		12 (11)	12 (12)		10 (11)	6 (8.7)	2 (9.1)	6 (20)	
Diabetes [n (%)]			0.3			0.5					0.3
No	137 (88)	48 (92)		95 (87)	90 (91)		74 (85)	63 (91)	21 (95)	27 (90)	
Yes	18 (12)	3 (5.8)		12 (11)	9 (9.1)		12 (14)	6 (8.7)	0 (0)	3 (10)	
Unknown	1 (0.6)	1 (1.9)		2 (1.8)	0 (0)		1 (1.1)	0 (0)	1 (4.5)	0 (0)	
Family history of premature CAD [n (%)]			0.8			**0.039**					0.2
No	70 (45)	26 (50)		42 (39)	54 (55)		32 (37)	38 (55)	10 (45)	16 (53)	
Yes	75 (48)	22 (42)		56 (51)	41 (41)		47 (54)	28 (41)	9 (41)	13 (43)	
Unknown	11 (7.1)	4 (7.7)		11 (10)	4 (4)		8 (9.2)	3 (4.3)	3 (14)	1 (3.3)	
Sexual orientation [n (%)]			**<0.001**			**0.041**					**<0.001**
Bisexual	12 (7.7)	0 (0)		7 (6.4)	5 (5.1)		7 (8.0)	5 (7.2)	0 (0)	0 (0)	
Heterosexual	38 (24)	40 (77)		32 (29)	46 (46)		15 (17)	23 (33)	17 (77)	23 (77)	
Homosexual (MSM)	106 (68)	12 (23)		70 (64)	48 (48)		65 (75)	41 (59)	5 (23)	7 (23)	
Ethnicity [n (%)]			0.19			**0.0042**					**0.009**
Caucasian	128 (82)	48 (92)		99 (90.8)	77 (77)		78 (89.6)	50 (72.4)	21 (95.4)	27 (90)	
Asian	3 (1.9)	0 (0)		3 (2.7)	0 (0)		3 (3.4)	0 (0)	0 (0)	0 (0)	
Black/Caribbean	16 (10.2)	1 (1.9)		5 (4.5)	12 (12)		4 (4.5)	12 (17)	1 (4.5)	0 (0)	
Black/African	1 (0.6)	1 (1.9)		0 (0)	2 (2)		0 (0)	1 (1.4)	0 (0)	1 (3.3)	

(*Continued on next page*)

Table 1. *Continued*

	HIV+ *N* = 156	HIV− *N* = 52	*p* value[a]	CAD+ *N* = 109	CAD− *N* = 99	*p* value[a]	HIV+CAD+ *N* = 87	HIV+CAD− *N* = 69	HIV−CAD+ *N* = 22	HIV−CAD− *N* = 30	*p* value[b]
Latino	8 (5.1)	2 (3.8)		2 (1.8)	8 (8)		2 (2.2)	6 (8.6)	0 (0)	2 (6.6)	
History of tobacco smoking [n (%)]			**0.031**			**0.001**					**0.004**
Current smoker	49 (31)	7 (13)		39 (36)	17 (17)		34 (39)	15 (22)	5 (23)	2 (6.7)	
Ex-smoker	58 (37)	21 (40)		42 (39)	37 (37)		33 (38)	25 (36)	9 (41)	12 (40)	
Never smoked	48 (31)	24 (46)		27 (25)	45 (45)		19 (22)	29 (42)	8 (36)	16 (53)	
Unknown	1 (0.6)	0 (0)		1 (0.9)	0 (0)		1 (1)	0 (0)	0 (0)	0 (0)	
Cigarette packs-years [Median (IQR)]	6 (0–26)	1 (0–13)	**0.017**	12 (0–27)	1 (0–15)	**<0.001**	13 (1–30)	1 (0–16)	5 (0–19)	0 (0–5)	**<0.001**
Cannabis use [n (%)]			**0.006**			>0.9					0.10
Active user	41 (26)	4 (7.7)		24 (22)	21 (21)		23 (26)	18 (26)	1 (4.5)	3 (10)	
Former user	12 (7.7)	8 (15)		11 (10)	9 (9.1)		7 (8.0)	5 (7.2)	4 (18)	4 (13)	
Non-user	103 (66)	40 (77)		74 (68)	69 (70)		57 (66)	46 (67)	17 (77)	23 (77)	
Alcohol units per week [Median (IQR)]	1 (0–6)	4 (1–6)	0.13	2 (0–6)	3 (0–6)	0.6	1 (0–6)	2 (0–6)	3 (0–7)	4 (1–6)	0.5
Type of alcohol drinker [n (%)]			0.11			0.068					0.2
Do not drink	48 (31)	12 (23)		33 (30)	27 (27)		27 (31)	21 (30)	6 (27)	6 (20)	
Ex-drinker	9 (5.8)	0 (0)		7 (6.4)	2 (2.0)		7 (8.0)	2 (2.9)	0 (0)	0 (0)	
Excessive drinker	11 (7.1)	2 (3.8)		10 (9.2)	3 (3.0)		8 (9.2)	3 (4.3)	2 (9.1)	0 (0)	
Social drinker	88 (56)	38 (73)		59 (54)	67 (68)		45 (52)	43 (62)	14 (64)	24 (80)	
Illicit drug use ever [n (%)]	70 (45)	14 (27)	**0.023**	49 (45)	35 (35)	0.2	43 (49)	27 (39)	6 (27)	8 (27)	0.070
Illicit drug use current [n (%)]	49 (31)	4 (7.7)	**<0.001**	32 (29)	21 (21)	0.2	31 (36)	18 (26)	1 (4.5)	3 (10)	**0.002**
Statin use [n (%)]			0.7			**0.007**					0.065
No	115 (74)	42 (81)		73 (67)	84 (85)		56 (64)	59 (86)	17 (77)	25 (83)	
Yes	36 (23)	9 (17)		31 (28)	14 (14)		27 (31)	9 (13)	4 (18)	5 (17)	
Unknown	5 (3.2)	1 (1.9)		5 (4.6)	1 (1.0)		4 (4.6)	1 (1.4)	1 (4.5)	0 (0)	
BMI [n (%)]			0.053			0.11					0.068
Healthy weight (18.5–25)	67 (43)	13 (25)		49 (45)	31 (31)		42 (48)	25 (36)	7 (32)	6 (20)	
Underweight (under 18.5)	7 (4.9)	1 (1.9)		5 (4.6)	3 (3.0)		4 (4.6)	3 (4.3)	1 (4.5)	0 (0)	
Overweight (over 25)	76 (49)	34 (65)		49 (45)	61 (62)		36 (41)	40 (58)	13 (59)	21 (70)	
Unknown	6 (3.8)	4 (7.7)		6 (5.5)	4 (4.0)		5 (5.7)	1 (1.4)	1 (4.5)	3 (10)	
Systolic blood pressure (mmHg) [Median (IQR)]	126 (112–134)	123 (117–132)	0.8	124 (111–136)	126 (117–133)	>0.9	124 (111–137)	126 (114–133)	120 (110–130)	126 (120–132)	0.9

(*Continued on next page*)

Table 1. *Continued*

	HIV+ *N* = 156	HIV− *N* = 52	*p* value[a]	CAD+ *N* = 109	CAD− *N* = 99	*p* value[a]	HIV+CAD+ *N* = 87	HIV+CAD− *N* = 69	HIV−CAD+ *N* = 22	HIV−CAD− *N* = 30	*p* value[b]
Framingham score [Median (IQR)]	9 (6–13)	8 (7–13)	0.5	10 (7–14)	8 (5–12)	**0.018**	9 (6–14)	8 (5–13)	12 (7–15)	7 (6–12)	0.063
Fasting glucose (mmol/L) [Median (IQR)]	5.00 (4.5–5.6)	4.9 (4.4–5.4)	0.3	5.0 (4.5–5.6)	5.00 (4.5–5.4)	0.4	5.10 (4.57–5.73)	5.00 (4.50–5.43)	4.90 (4.40–5.43)	4.95 (4.55–5.32)	0.5
Hb_A1c [Median (IQR)]	5.31 (5.07–5.7)	5.3 (5.09–5.52)	0.8	5.36 (5.10–5.60)	5.3 (4.96–5.60)	0.3	5.35 (5.10–5.70)	5.30 (5.00–5.70)	5.37 (5.25–5.50)	5.30 (4.81–5.52)	0.7
Total cholesterol (mmol/L) [Median (IQR)]	4.75 (4.16–5.38)	5.07 (4.6–5.47)	**0.039**	4.77 (4.16–5.47)	4.99 (4.32–5.35)	0.2	4.67 (4.12–5.50)	4.88 (4.26–3.20)	4.98 (4.66–5.44)	5.22 (4.57–5.67)	0.2
LDL (mmol/L) [Median (IQR)]	2.61 (2.05–3.2)	3.06 (2.68–3.52)	**0.002**	2.63 (2.08–3.21)	2.92 (2.32–3.37)	0.082	2.54 (1.91–3.20)	2.76 (2.26–3.20)	3.00 (2.68–3.39)	3.12 (2.73–3.57)	**0.007**
HDL (mmol/L) [Median (IQR)]	1.18 (0.97–1.4)	1.36 (1.18–1.56)	**0.004**	1.20 (0.97–1.45)	1.24 (1.03–1.45)	0.4	1.16 (0.95–1.42)	1.21 (1.01–1.39)	1.35 (1.18–1.58)	1.38 (1.14–1.51)	**0.026**
LDL:HDL ratio [Median (IQR)]	2.16 (1.63–2.88)	2.21 (1.83–2.87)	0.3	2.15 (1.61–2.95)	2.19 (1.75–2.86)	0.7	2.16 (1.57–2.95)	2.16 (1.71–2.83)	2.14 (1.83–2.67)	2.22 (1.82–2.89)	0.8
Triglyceride (mmol/L) [Median (IQR)]	1.70 (1.02–2.28)	1.35 (0.93–1.96)	**0.050**	1.81 (1.02–2.22)	1.38 (0.97–2.07)	**0.037**	1.92 (1.07–2.50)	1.45 (0.97–2.04)	1.41 (0.92–1.91)	1.31 (0.95–2.10)	**0.022**
Insulin (pmol/L) [Median (IQR)]	76 (46–140)	55 (46–77)	**0.013**	71 (42–127)	71 (50–112)	0.7	75 (42–141)	76 (55–126)	58 (45–81)	53 (46–72)	0.081

HIV, human immunodeficiency virus; CAD, coronary artery disease; CMV-IgG, immunoglobulin G specific for cytomegalovirus; BMI, body mass index; Hb-A1c, hemoglobin A1c; LDL, low-density lipoprotein; HDL, high-density lipoprotein; mmHg.

[a]Fisher's exact test; Mann–Whitney *U* test.

[b]Fisher's exact test for count data; Kruskal-Wallis rank-sum test; Significant values are presented in bold.

Table 2. Endocannabinoids and endocannabinoid-like lipids in participants according to their HIV and subclinical coronary artery disease status

	HIV+ [Median (pmol/μL) (IQR)]	HIV− [Median (pmol/μL) (IQR)]	*p* value[a] (HIV+ vs. HIV−)	CAD+ [Median (pmol/μL) (IQR)]	CAD− [Median (pmol/μL) (IQR)]	*p* value[a] (CAD+ vs. CAD−)
N-acyl-ethanolamines (NAEs)						
AEA	0.01042 (0.007–0.013)	0.01277 (0.008–0.015)	**0.018**	0.01029 (0.007–0.013)	0.01151 (0.008–0.014)	NS
EPEA	0.0001417 (0.000–0.0002)	0.000199 (0.00014–0.0003)	**<0.0001**	0.00014 (0.000–0.00019)	0.0001821 (0.00011–0.00025)	**0.013**
LEA	0.001595 (0.00122–0.0021)	0.001844 (0.0014–0.0024)	**0.017**	0.001636 (0.0012–0.0021)	0.001650 (0.00127–0.0023)	NS
DHEA	0.002214 (0.0017–0.0027)	0.002471 (0.0019–0.0031)	**0.032**	0.002117 (0.0016–0.0027)	0.002474 (0.0018–0.0028)	**0.028**
PEA	0.001404 (0.0011–0.0019)	0.0015 (0.0011–0.0022)	NS	0.00139 (0.0011–0.0018)	0.001499 (0.0011–0.0021)	NS
OEA	0.007316 (0.0056–0.0089)	0.00779 (0.0063–0.0096)	NS	0.00733 (0.0054–0.0091)	0.007322 (0.0062–0.0091)	NS
SEA	0.007776 (0.0063–0.0101)	0.007936 (0.0067–0.0096)	NS	0.007851 (0.00633–0.0099)	0.007746 (0.0066–0.0098)	NS
DPA-EA(n-6)	0.0007618 (0.00054–0.00102)	0.0009496 (0.00069–0.00116)	**0.013**	0.0007417 (0.00052–0.00104)	0.0008668 (0.00060–0.00112)	NS
DPA-EA(n-3)	0.0002728 (0.00018–0.00036)	0.0002330 (0.00019–0.00031)	NS	0.0002712 (0.00019–0.00036)	0.0002657 (0.00018–0.00032)	NS
Monoacylglycerols (MAGs)						
2-AG	0.1257 (0.0392–0.2462)	0.07797 (0.030–0.1844)	0.096	0.1276 (0.04143–0.2476)	0.07844 (0.0327–0.2028)	NS
2-EPG	0.002059 (0.00131–0.00378)	0.001590 (0.00092–0.00283)	**0.015**	0.002064 (0.00127–0.00361)	0.001812 (0.00111–0.00326)	NS
2-DHG	0.008028 (0.00511–0.01411)	0.006415 (0.00482–0.01016)	0.079	0.008037 (0.00507–0.01399)	0.007394 (0.00477–0.01153)	NS
2-LG	0.1026 (0.05948–0.1611)	0.06861 (0.04553–0.1050)	**0.0004**	0.09859 (0.05738–0.1478)	0.08395 (0.05469–0.1438)	NS
2-DPG	0.02282 (0.01427–0.03388)	0.01647 (0.01124–0.02428)	**0.0035**	0.02119 (0.01416–0.03397)	0.01943 (0.01328–0.03082)	NS
2-OG	0.1101 (0.06536–0.1615)	0.06698 (0.04853–0.1208)	**0.0007**	0.1125 (0.06672–0.1542)	0.08480 (0.05154–0.1419)	**0.031**

(*Continued on next page*)

Table 2. *Continued*

	HIV+ [Median (pmol/μL) (IQR)]	HIV− [Median (pmol/μL) (IQR)]	*p* value[a] (HIV+ vs. HIV−)	CAD+ [Median (pmol/μL) (IQR)]	CAD− [Median (pmol/μL) (IQR)]	*p* value[a] (CAD+ vs. CAD−)
Polyunsaturated fatty acid (PUFA)						
SDA	0.3499 (0.1522–0.6470)	0.3495 (0.1069–0.4985)	NS	0.3821 (0.1608–0.6518)	0.3426 (0.1114–0.5579)	NS
EPA	0.4504 (0.2895–0.6602)	0.4531 (0.3370–0.6911)	NS	0.4242 (0.2793–0.6251)	0.4610 (0.3473–7186)	NS
DHA	1.592 (1.055–2.415)	1.462 (1.208–2.248)	NS	1.480 (1.072–2.077)	1.730 (1.193–2.564)	NS
AA	2.555 (1.973–3.382)	2.277 (1.871–2.797)	NS	2.290 (1.933–3.059)	2.555 (2.017–3.258)	NS
DPA n-3	0.1640 (0.1013–0.2294)	0.1319 (0.08607–0.1716)	**0.014**	0.1500 (0.09297–0.2288)	0.1525 (0.1028–0.1997)	NS
DPA n-6	0.6415 (0.4080–0.9033)	0.5606 (0.3961–0.7755)	NS	0.5680 (0.3696–0.8391)	0.6485 (0.4224–0.9030)	NS
LA	19.98 (14.62–26.11)	18.99 (13.18–24.46)	NS	19.66 (13.89–23.75)	19.98 (14.94–27.42)	NS

AEA, *N*-arachidonoylethanolamine; EPEA, *N*-eicosapentaenoylethanolamine; LEA, *N*-linoleoylethanolamine; DHEA, *N*-docosahexaenoylethanolamine; PEA, *N*-palmitoylethanolamine; OEA, *N*-oleoylethanolamine; SEA, *N*-stearoylethanolamine; DPA-EA(n-6), *N*-docosapentaenoylethanolamine n-6; DPA-EA(n-3), *N*-docosapentaenoylethanolamine n-3; 2-AG, 2-arachidonoylglycerol; 2-EPG, 2-eicosapentaenoylglycerol; 2-DHG, 2-docosahexaenoylglycerol; 2-LG, 2-linoleoylglycerol; 2-DPG, 2-docosapentaenoylglycerol n-3; 2-OG, 2-oleoylglycerol; SDA, stearidonic acid; EPA, eicosapentaenoic acid; DHA, docosahexaenoic acid; AA, arachidonic acid; DPA-ω 3, docosapentaenoic acid n-3; DPA-ω 6, docosapentaenoic acid n-6; LA, linoleic acid; PUFA, polyunsaturated fatty acid; HIV, human immunodeficiency virus; CAD, coronary artery disease.

[a]Mann-Whitney U test; Significant values are presented in bold; NS: Not significant.

N-eicosapentaenoylethanolamine (EPEA), *N*-linoleoylethanolamine (LEA), *N*-docosahexaenoylethanolamine (DHEA), *N*-palmitoylethanolamine (PEA), *N*-oleoylethanolamine (OEA), *N*-stearidonoylethanolamine (SEA), *N*-docosapentaenoylethanolamine n-6 [DPA-EA(n-6)], and *N*-docosapentaenoylethanolamine n-3 [DPA-EA(n-3)]. The second group was composed of 2-monoacylglycerols (MAGs), including the eCB 2-arachidonoylglycerol (2-AG) and its congeners, 2-eicosapentaenoylglycerol (2-EPG), 2-docosahexaenoylglycerol (2-DHG), 2-linoleoylglycerol (2-LG), 2-docosapentaenoylglycerol n-3 (2-DPG), and 2-oleoylglycerol (2-OG). We also analyzed the levels of polyunsaturated fatty acids (PUFAs), including stearidonic acid (SDA), eicosapentaenoic acid (EPA), docosahexaenoic acid (DHA), arachidonic acid (AA), n-3 docosapentaenoic acid (DPA n-3), n-6 docosapentaenoic acid (DPA n-6), and linoleic acid (LA). The changes in the plasma levels of these lipids are detailed in Tables 2 and 3. Overall, we observed a peculiar pattern with an inverse relationship in plasma levels between NAEs and MAGs (including the two eCBs AEA and 2-AG), with NAEs being most significantly elevated in HIV− individuals as well as in CAD− participants and MAGs being most significantly elevated in HIV+ and in individuals with CAD (Table 2).

N-acylethanolamines

AEA ($p = 0.018$), EPEA ($p < 0.0001$), LEA ($p = 0.017$), DHEA ($p = 0.03$), and DPA-EA(n-6) ($p = 0.013$) were significantly lower in PWH compared to HIV− participants, and the other NAEs followed the same pattern but without statistically significant differences (Table 2). When considering only CAD, AEA and several other NAE lipids [LEA, PEA, OEA, DPA-EA(n-6)] were lower in CAD+ compared to CAD− individuals, but without reaching the statistical significance. However, EPEA and DHEA, which were significantly lower in HIV+ compared to HIV− individuals, were similarly lower in CAD+ compared to CAD− individuals ($p = 0.01$ and $p = 0.03$, respectively, Table 2). Within HIV+ participants, EPEA ($p = 0.04$), DHEA ($p = 0.018$), and PEA ($p = 0.03$) were significantly elevated in HIV+CAD− compared to HIV+CAD+ subgroup, whereas AEA and its other congeners did not show any statistical difference (Table 3). Within HIV− participants, no significant difference was observed in the plasma concentrations of AEA and its congeners between participants with and without CAD (Table 3). On the other hand, most of the NAEs, including AEA ($p = 0.02$), EPEA ($p < 0.0001$), LEA ($p = 0.02$), DHEA ($p = 0.02$), and DPA-EA(n-6) ($p = 0.02$), were significantly reduced in the HIV+CAD+ compared to the HIV−CAD− controls (Table 3). The other congeners of AEA followed the same pattern, but without reaching statistical significance. Several NAEs were either significantly reduced (EPEA [$p = 0.005$], DHEA [$p = 0.02$]) or tended to be so [LEA, PEA, and DPA-EA(n-6)] in the HIV+CAD+ compared to HIV−CAD+ participants (Table 3). Finally, only EPEA ($p = 0.01$) was significantly reduced in HIV+CAD− compared to the HIV−CAD− individuals (Table 3).

Monoacylglycerols

Contrary to what was observed for NAEs, 2-EPG ($p = 0.02$), 2-LG ($p = 0.0004$), 2-DPG ($p = 0.0035$), and 2-OG ($p = 0.0007$) were significantly elevated in HIV+ versus HIV− participants, with a tendency of elevated plasma levels of 2-AG and 2-DHG ($p = 0.09$ and $p = 0.07$, respectively) (Table 2). When considering only CAD status, although all MAGs had the tendency to be increased in CAD+ compared to CAD− participants, only 2-OG reached statistical significance ($p = 0.03$, Table 2). Although plasma levels of 2-AG and several of its congeners were elevated in the HIV+CAD+ compared to the HIV+CAD−individuals, here again, only 2-OG ($p = 0.02$) reached statistical significance (Table 3). When comparing HIV+CAD+ versus HIV−CAD+, all MAGs, including 2-AG ($p = 0.04$), 2-EPG ($p = 0.02$), 2-LG ($p = 0.004$), 2-DPG ($p = 0.01$), 2-OG ($p = 0.001$), and 2-DHG ($p = 0.08$), were elevated in HIV+CAD+ participants (Table 3). The same pattern was maintained for several MAGs between the HIV+CAD+ versus the HIV−CAD− subgroup, with 2-EPG ($p = 0.04$), 2-LG ($p = 0.006$), 2-DPG ($p = 0.03$), and 2-OG ($p = 0.003$) being significantly elevated in HIV+CAD+ participants (Table 3). The 2-LG ($p = 0.02$) and 2-DPG ($p = 0.04$) were significantly elevated in the HIV+CAD− compared to the HIV−CAD+ group, and only 2-LG ($p = 0.04$) was significantly elevated in the HIV+CAD− compared to HIV−CAD− subgroup. Within HIV− participants, no significant pattern was observed in the plasma levels of MAGs (Table 3).

Polyunsaturated fatty acids

Overall, no particular pattern was observed in the plasma levels of PUFAs when considering either the HIV or CAD status only; nevertheless, DPA n-3 was significantly elevated in HIV+ versus HIV− participants ($p = 0.02$) (Table 3). In addition, DPA n-3 ($p = 0.04$), AA ($p = 0.04$), and DPA n-6 ($p = 0.06$) were significantly, or tended to be, elevated in the HIV+CAD− compared to the HIV−CAD+ subgroup. DPA n-3 only tended to be elevated in the HIV+CAD+ compared to the HIV−CAD+ subgroup ($p = 0.07$), as well as in the HIV+CAD− compared to the HIV−CAD− subgroup ($p = 0.09$) (Table 3).

Changes in fecal microbiota in people with HIV and subclinical coronary artery disease

Gut microbiota profiles were assessed in stool samples from a subset of study participants ($n = 107$) for whom the stool specimens were available including HIV+CAD+ ($n = 39$), HIV+CAD− ($n = 26$), HIV−CAD+ ($n = 19$), and HIV−CAD− ($n = 23$). Beta diversity of the gut microbiota was assessed by principal-component analysis (PCA) at the family and genus taxonomic levels, which did not result in separate clusters based on the CAD or HIV status (Figure S1). Similarly, principal coordinates analysis (PCoA) followed by PERMANOVA was not able to distinguish between the CAD− and CAD+ groups (Figure 1A). However, although the HIV− and HIV+ groups largely overlapped, PERMANOVA analysis identified significant differences between the groups ($p < 0.001$; Figure 1B). Similarly, when the participants were separated into four groups based on their HIV and CAD status, once again, the centroids overlapped significantly, and subsequent PERMANOVA found a significant difference ($p < 0.001$; Figure 1C). However, an additional post-hoc analysis failed to identify differences between the individual groups. As

Table 3. Comparison of endocannabinoids and endocannabinoid-like lipids in participants according to their HIV and subclinical coronary artery disease status

	HIV+CAD+ [Median (pmol/μL) (IQR)]	HIV+CAD− [Median (pmol/μL) (IQR)]	HIV−CAD+ [Median (pmol/μL) (IQR)]	HIV−CAD− [Median (pmol/μL) (IQR)]	Kruskal-Wallis p-value[b]	p value[a] HIV+CAD+ vs. HIV+CAD−	p value[a] HIV−CAD+ vs. HIV+CAD+	p value[a] HIV+CAD+ vs. HIV−CAD−	p value[a] HIV−CAD+ vs. HIV+CAD−	p value[a] HIV−CAD− vs. HIV+CAD−	p value[a] HIV−CAD− vs. HIV−CAD+
N-Acyl-ethanolamines (NAEs)											
AEA	0.01013 (0.00771–0.01299)	0.01083 (0.00843–0.01373)	0.01277 (0.00811–0.01591)	0.01289 (0.00877–0.01556)	0.08	NS	NS	**0.017**	NS	NS	NS
EPEA	0.0001271 (0.00008–0.00019)	0.0001691 (0.00011–0.00022)	0.0001899 (0.00013–0.00033)	0.0002102 (0.00016–0.00028)	**0.0002**	**0.042**	**0.005**	**<0.0001**	NS	**0.01**	NS
LEA	0.001600 (0.00122–0.00201)	0.001572 (0.00121–0.00215)	0.001973 (0.00129–0.00244)	0.001810 (0.00151–0.00251)	NS	NS	0.097	**0.023**	NS	NS	NS
DHEA	0.002041 (0.00156–0.00269)	0.002474 (0.00182–0.00285)	0.002471 (0.00203–0.00361)	0.002449 (0.00182–0.00294)	**0.013**	**0.018**	**0.015**	**0.018**	NS	NS	NS
PEA	0.001310 (0.00105–0.00171)	0.001567 (0.00114–0.00215)	0.001605 (0.00114–0.00266)	0.001415 (0.00111–0.00226)	0.07	**0.034**	0.081	NS	NS	NS	NS
OEA	0.007319 (0.00534–0.00883)	0.007156 (0.00620–0.00896)	0.007792 (0.00653–0.00956)	0.007516 (0.00614–0.00974)	NS	NS	NS	NS	NS	NS	NS
SEA	0.007905 (0.00632–0.00993)	0.007637 (0.00647–0.0101)	0.007636 (0.00673–0.01002)	0.008204 (0.00673–0.00933)	NS	NS	NS	NS	NS	NS	NS
DPA-EA(n-6)	0.0007078 (0.00051–0.00096)	0.0008175 (0.00057–0.00106)	0.0009199 (0.00063–0.00124)	0.009608 (0.00073–0.00114)	NS	NS	0.084	**0.013**	NS	NS	NS
DPA-EA(n-3)	0.0002827 (0.00021–0.00037)	0.0002667 (0.00017–0.00034)	0.0002195 (0.00018–0.00033)	0.0002555 (0.00021–0.00032)	NS	NS	NS	NS	NS	NS	NS
Monoacylglycerols (MAGs)											
2-AG	0.1379 (0.0469–0.2718)	0.1137 (0.03273–0.2015)	0.08092 (0.02381–0.1474)	0.07473 (0.03152–0.2059)	0.054	NS	**0.046**	NS	NS	NS	NS
2-EPG	0.002119 (0.00147–0.00407)	0.001875 (0.00112–0.00332)	0.001532 (0.00067–0.00265)	0.001625 (0.00105–0.00291)	**0.013**	NS	**0.020**	**0.044**	NS	NS	NS
2-DHG	0.008514 (0.00543–0.01448)	0.007654 (0.00456–0.01386)	0.006264 (0.00396–0.01257)	0.006815 (0.00495–0.01006)	0.067	NS	0.083	NS	NS	NS	NS
2-LG	0.1161 (0.06012–0.1759)	0.09692 (0.05930–0.1531)	0.06595 (0.0400–0.1017)	0.07304 (0.04693–0.1052)	**0.0006**	NS	**0.003**	**0.007**	**0.023**	**0.044**	NS
2-DPG	0.02376 (0.01518–0.03679)	0.02071 (0.01370–0.03207)	0.01735 (0.01115–0.2057)	0.01634 (0.01179–0.02667)	**0.006**	NS	**0.011**	**0.027**	**0.046**	NS	NS
2-OG	0.1193 (0.08917–0.1754)	0.08959 (0.05410–0.1522)	0.06698 (0.04404–0.1125)	0.06825 (0.04893–0.1250)	**0.0002**	**0.022**	**0.001**	**0.002**	NS	NS	NS
Polyunsaturated fatty acid (PUFA)											
SDA	0.3953 (0.1637–0.6952)	0.3109 (0.1110–0.5700)	0.3459 (0.06879–0.5529)	0.3543 (0.1216–0.5104)	NS	NS	NS	NS	NS	NS	NS

(*Continued on next page*)

Table 3. *Continued*

	HIV+CAD+ [Median (pmol/μL) (IQR)]	HIV+CAD− [Median (pmol/μL) (IQR)]	HIV−CAD+ [Median (pmol/μL) (IQR)]	HIV−CAD− [Median (pmol/μL) (IQR)]	Kruskal-Wallis *p*-value[b]	*p* value[a] HIV+CAD+ vs. HIV+CAD−	*p* value[a] HIV−CAD+ vs. HIV+CAD+	*p* value[a] HIV+CAD+ vs. HIV−CAD−	*p* value[a] HIV−CAD+ vs. HIV+CAD−	*p* value[a] HIV−CAD− vs. HIV+CAD−	*p* value[a] HIV−CAD− vs. HIV−CAD+
EPA	0.4187 (0.2756–0.6269)	0.4707 (0 0.3151–0.7074)	0.4242 (0.2932–0.6046)	0.4605 (0.3490–0.7243)	NS	NS	NS	NS	NS	NS	NS
DHA	1.485 (1.055–2.041)	1.753 (1.056–2.573)	1.413 (1.165–2.279)	1.509 (1.204–2.282)	NS	NS	NS	NS	NS	NS	NS
AA	2.313 (1.939–3.361)	2.604 (2.045–3.426)	2.095 (1.868–2.623)	2.370 (1.888–3.014)	NS	NS	NS	NS	**0.042**	NS	NS
DPA n-3	0.1564 (0.09885–0.2371)	0.1650 (0.1067–0.2016)	0.1218 (0.07622–0.1623)	0.1369 (0.09649–0.1859)	**0.024**	NS	0.072	NS	**0.039**	0.095	NS
DPA *n*-6	0.6200 (0.3665–0.8680)	0.6630 (0.4300–0.9827)	0.4597 (0.3610–0.6601)	0.6084 (0.4110–0.8268)	NS	NS	NS	NS	0.0628	NS	NS
LA	19.62 (14.34–24.14)	20.31 (14.88–28.83)	19.73 (12.36–23.45)	18.83 (14.59–25.04)	NS	NS	NS	NS	NS	NS	NS

AEA, *N*-arachidonoylethanolamine; EPEA, *N*-eicosapentaenoylethanolamine; LEA, *N*-linoleoylethanolamine; DHEA, *N*-docosahexaenoylethanolamine; PEA, *N*-palmitoylethanolamine; OEA, *N*-oleoylethanolamine; SEA, *N*-stearoylethanolamine; DPA-EA(n-6), *N*-docosapentaenoylethanolamine n-6; DPA-EA(n-3), *N*-docosapentaenoylethanolamine n-3, 2-AG, 2-arachidonoylglycerol; 2-EPG, 2-eicosapentaenoylglycerol; 2-DHG, 2-docosahexaenoylglycerol; 2-LG, 2-linoleoylglycerol; 2-DPG, 2-docosapentaenoylglycerol n-3; 2-OG, 2-oleoylglycerol; SDA, stearidonic acid; EPA, eicosapentaenoic acid; DHA, docosahexaenoic acid; AA, arachidonic acid; DPA-ω 3, docosapentaenoic acid n-3; DPA-ω 6, docosapentaenoic acid n-6; LA, linoleic acid; PUFA, polyunsaturated fatty acid; HIV, human immunodeficiency virus; CAD, coronary artery disease.

[a]Mann-Whitney U test; significant values are presented in bold; NS: not significant.

[b]Kruskal-Wallis rank-sum test.

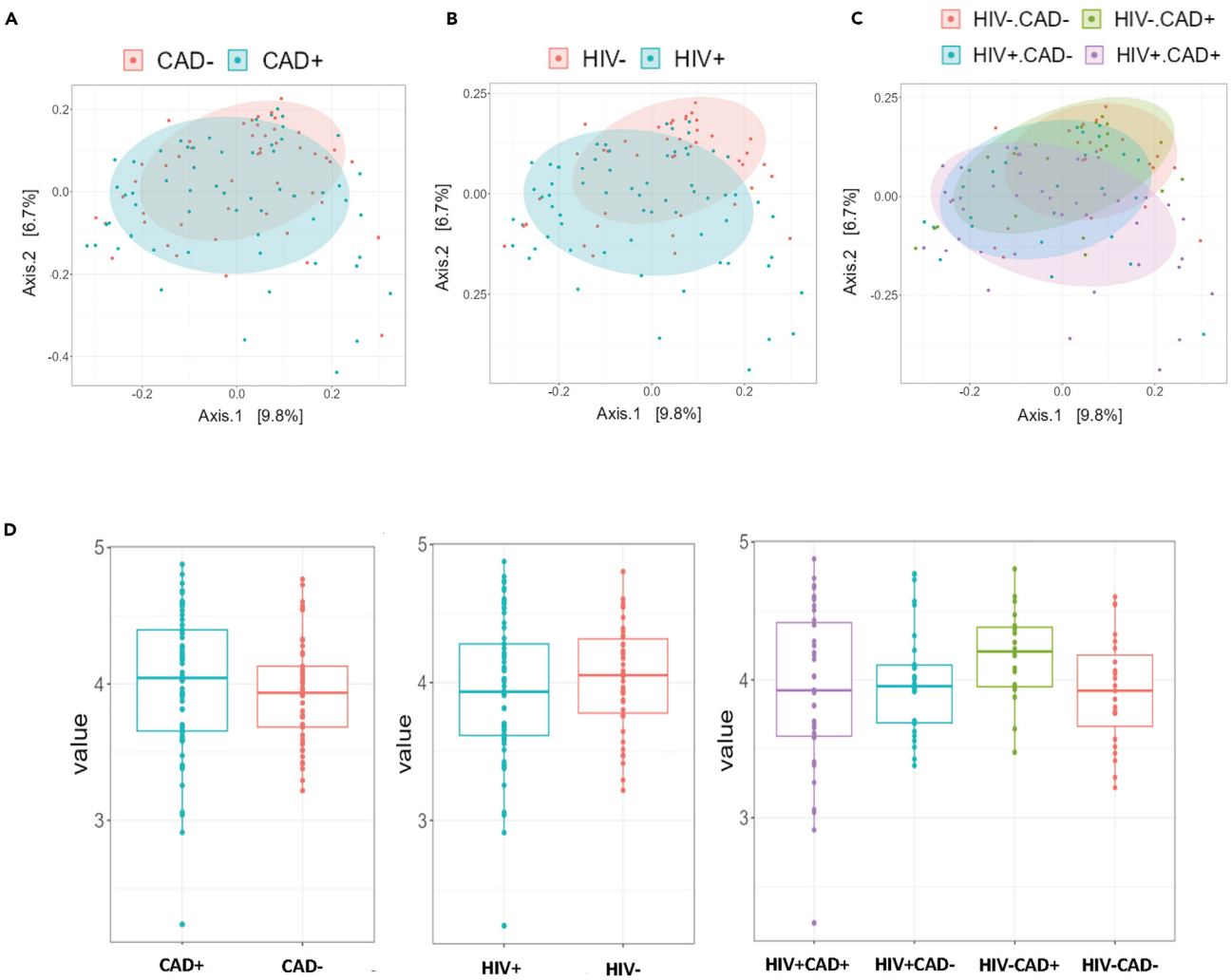

Figure 1. Principal coordinate analysis (PCoA) and Shannon alpha-diversity index representation of gut microbiotas from study participants according to HIV and coronary artery disease (CAD)

(A) PCoA analysis according to CAD status. Red dots correspond to participants without CAD, whereas blue dots correspond to CAD+ participants.

(B) PCoA analysis according to HIV status. Red dots correspond to HIV− participants, whereas blue dots correspond to HIV+ participants.

(C) PCoA analysis integrating both HIV and CAD status. Red dots correspond to HIV−CAD−participants, blue dots correspond to HIV+CAD− participants, green dots correspond to HIV−CAD+ participants, and purple dots correspond to HIV+CAD+ participants.

(D) Shannon alpha-diversity index representation. The graph on the left corresponds to the CAD status. The graph in the middle corresponds to HIV status. The graph on the right corresponds to both HIV and CAD status.

it might be expected from the aforementioned findings, no differences in Shannon alpha diversity were identified when comparing the CAD− and CAD+, the HIV−, and HIV+ groups, nor the four groups based on their HIV and CAD status (Figure 1D).

The abundance of different families and genera of the fecal microbiota of the study participants was then determined to identify taxa that were differentially abundant in the four study groups. We globally observed an alteration of profiles of the bacterial families found in HIV−CAD− controls in favor of an increase in their proportion in HIV−CAD+ (although not statistically significant for most of them), whereas the abundance of most of these bacterial families was drastically reduced in HIV+CAD+ (Table 4). Indeed, compared to healthy HIV−CAD−controls, HIV−CAD+ carried significantly more *Marinifilaceae* (p = 0.03) and almost significantly more *Sutterellaceae* (p = 0.08); the other bacterial families also followed the same trend, but without reaching the statistical significance. On the other hand, *Bacteroidaceae* (p = 0.01), *Ruminococcaceae* (p = 0.0003), *Monoglobaceae* (p = 0.03), *Sutterellaceae* (p = 0.017), and *Marinifilaceae* (p = 0.007) were found to be significantly depleted in HIV+CAD+ compared to HIV−CAD+ (Table 4). Similarly, *Bacteroidaceae* (p = 0.03), *Ruminococcaceae* (p = 0.03), *Marinifilaceae* (p = 0.022), and *Monoglobaceae* (p = 0.07) were also significantly depleted in HIV+CAD− compared to HIV−CAD+ (Table 4). Regarding the different genera of bacterial microbiota, a similar trend to what was observed for bacterial families was also found; with increased abundance in HIV−CAD+ compared to HIV−CAD− healthy controls and reversal of this trend in HIV+CAD+. Indeed,

Table 4. Changes in the abundance of bacterial families and genera of the fecal microbiota in PWH with subclinical coronary artery disease

	HIV−CAD+ vs. HIV−CAD−	HIV+CAD− vs. HIV−CAD−	HIV+CAD+ vs. HIV−CAD−	HIV+CAD− vs. HIV−CAD+	HIV+CAD+ vs. HIV−CAD+	HIV+CAD+ vs. HIV+CAD−
Family [difference of means (95% family-wide confidence level range)]						
Bacteroidaceae	9.65 (−14.29 to 33.61)	−15.61 (−37.73 to 6.51)	−16.60 (-36.92–3.71)	**−25.27* (−48.59 to −1.94)**	**−26.26* (−47.88 to −4.64)**	−0.99 (−20.56 to 18.57)
Ruminococcaceae	17.08 (−6.56 to 40.74)	−7.64 (−29.44 to 14.16)	−17.68 (−37.57 to 2.20)	**−24.72* (−47.98 to −1.47)**	**−34.77*** (−56.23 to −13.30)**	−10.04 (−29.44 to 9.36)
Monoglobaceae	7.05 (−17.28 to 31.40)	−15.23 (−37.67 to 7.20)	−16.67 (−-37.13 to 3.79)	**−22.29* (−46.21 to 1.63)**	**−23.72* (−45.81 to −1.64)**	−1.43 (−21.40 to 18.53)
Sutterellaceae	19.26 (−1.64 to 40.16)	6.55 (−12.71 to 25.82)	−2.51 (−20.08 to 15.06)	−12.70 (−33.25 to 7.84)	**−21.77* (−40.74 to −2.80)**	−9.07 (−26.21 to 8.07)
Marinifilaceae	**23.43* (1.74–45.11)**	−0.31 (−20.29 to 19.67)	−1.51 (−19.73 to 16.72)	**−23.74* (−45.05 to −2.43)**	**−24.93** (−44.61 to −5.26)**	−1.19 (−18.98 to 16.59)
Genus [difference of means (95% family-wide confidence level range)]						
Bacteroides	9.65 (−14.29 to 33.61)	−15.61 (−37.73 to 6.51)	−16.60 (−36.92 to –3.71)	**−25.27* (−48.59 to −1.94)**	**−26.26* (−47.88 to −4.64)**	−0.99 (−20.56 to 18.57)
Butyricimonas	**16.99* (0.01–33.97)**	3.82 (−11.84 to 19.50)	1.57 (−12.82 to –15.96)	−13.16 (−29.63 to 3.36)	**−15.42* (−30.74 to −0.10)**	−2.25 (−16.12 to 11.60)
CAG-56	0.39 (−20.19 to 20.97)	**−23.37** (−42.38 to −4.36)**	12.70 (−30.15 to 4.75)	**−23.76* (−43.80 to −3.72)**	−13.09 (−31.67 to 5.48)	10.67 (−6.13 to 27.48)
Faecalibacterium	20.41 (−2.67 to 43.49)	−7.10 (−28.41 to 14.21)	−16.78 (−36.35 to 2.79)	**−27.51** (−40.99 to −5.04)**	**−37.19*** (−58.02 to −16.36)**	−9.67 (−28.53 to 9.17)
Flavonifractor	12.81 (−3.00 to 28.63)	6.06 (−8.54 to 20.67)	−3.72 (−17.14 to 9.69)	−6.74 (−22.15 to 8.65)	**−16.53* (−30.81 to −2.25)**	−9.78 (−22.71 to 3.13)
Lachnospira	**28.49** (6.37–50.61)**	−0.82 (−21.24 to 19.59)	−7.42 (−26.17 to 11.33)	**−29.32** (−50.85 to −7.79)**	**−35.91*** (−55.87 to −15.96)**	−6.59 (−24.65 to 11.46)
Lachnospiraceae_UCG-001	**27.96** (7.82–48.10)**	−2.81 (−21.41 to 15.77)	−10.61 (−27.68 to 6.46)	**−30.78*** (−50.38 to −11.17)**	**−38.57*** (−56.75 to 20.40)**	−7.79 (−24.23 to 8.65)
Lachnospiraceae_UCG-004	19.32 (−0.58 to 39.23)	1.03 (−17.34 to 19.41)	−10.22 (−27.10 to 6.65)	−18.29 (−37.67 to 1.08)	**−29.54*** (−47.51 to 11.58)**	−11.25 (−27.51 to 5.00)
Lachnospiraceae_NK4A136_group	12.90 (−11.13 to 36.95)	−15.85 (−37.78 to 6.62)	−10.15 (−30.55 to 10.23)	**−28.48* (−51.90 to −5.07)**	**−23.06* (−44.76 to −1.36)**	5.42 (−14.21 to 25.06)
Oscillibacter	**22.09* (0.78–43.41)**	1.32 (−18.36 to 21.01)	−6.75 (−24.83–11.32)	**−20.77* (−41.53 to −0.02)**	**−28.85*** (−48.09 to −-9.61)**	−8.07 (−25.48 to 25.06)
Roseburia	23.14 (−0.63 to 46.92)	−7.01 (−28.97 to 14.94)	−6.42 (−26.59 to 13.74)	**−30.15** (−53.31 to −7.00)**	**−29.56** (−51.02 to −8.10)**	0.58 (−18.83 to 20.01)

(*Continued on next page*)

Table 4. *Continued*

	HIV−CAD+ vs. HIV−CAD−	HIV+CAD− vs. HIV−CAD−	HIV+CAD+ vs. HIV−CAD−	HIV+CAD− vs. HIV−CAD+	HIV+CAD+ vs. HIV−CAD+	HIV+CAD+ vs. HIV+CAD−
Anaerosporobacter	−1.59 (−15.44 to 12.24)	**−16.04** (−28.82 to −3.25)**	**−13.33* (−25.08 to 1.59)**	**−14.44* (−27.92 to 0.96)**	−11.74 (−24.23 to −0.75)	2.71 (−8.60 to 14.01)
Blautia	**−26.14* (−50.62 to −1.65)**	−18.63 (−41.24 to 3.97)	−14.14 (−34.91 to 6.61)	7.51 (−16.33 to 31.34)	11.99 (−10.10 to 34.09)	4.48 (−15.51 to 24.48)
Fusicatenibacter	−15.59 (−38.62 to 7.44)	−13.71 (−34.98 to 7.55)	**−34.55*** (−54.08 to −15.02)**	1.87 (−20.54 to 24.29)	−18.96 (−39.74 to 1.82)	**−20.83* (−39.64 to 2.03)**
Erysipelotrichaceae_UCG-003	−10.17 (−33.84 to 13.48)	−16.95 (−38.80 to 4.89)	**−21.91* (−41.98 to −1.84)**	6.77 (−29.81 to 16.26)	−11.73 (−33.09 to 9.61)	−4.96 (−24.28 to 14.36)
Romboutsia	−6.74 (−30.59 to 17.11)	−17.80 (−39.83 to 4.21)	**−24.21* (−44.43 to −3.97)**	−11.06 (−34.28 to 12.15)	−17.46 (−38.98 to 4.06)	−6.39 (−25.87 to 13.08)
Subdoligranulum	−12.34 (−36.42 to 11.72)	**−24.62* (−46.84 to −2.39)**	**−24.80* (−45.22 to −4.39)**	−12.27 (−35.70 to 11.16)	−12.45 (−34.18 to 9.26)	−0.18 (−19.84 to 19.47)
Alloprevotella	3.98 (−17.60 to 25.56)	13.15 (−6.76 to 33.08)	**21.43* (3.13–39.73)**	9.17 (−11.83 to 30.19)	17.45 (−2.02 to 36.93)	8.27 (−9.35 to 25.90)
Catenisphaera	2.22 (−15.79 to 20.22)	7.46 (−9.16 to 24.09)	**16.84* (1.57–32.12)**	5.24 (−12.28 to 22.78)	14.63 (−1.62 to 30.88)	9.38 (−5.32 to 24.09)

Stool specimens were collected from HIV+CAD+ (n = 39), HIV+CAD− (n = 26), HIV−CAD+ (n = 19), and HIV−CAD− (n = 23).

Tukey multiple comparison of means 95% family-wide confidence level. Results are displayed as difference of means alongside the range (lower and upper values) of the 95% family-wide confidence level. Significant values are shown in bold (*$p < 0.05$; **$p < 0.01$; ***$p < 0.001$).

HIV−CAD+ carried significantly more *Butyricimonas* ($p = 0.049$), *Lachnospira* ($p = 0.005$), *Lachnospira*_UCG-001 ($p = 0.002$), *Oscillibacter* ($p = 0.04$), and *Roseburia* ($p = 0.05$) and showed trends toward harboring significantly more *Lachnospira*_UCG-004 ($p = 0.06$) and *Sutterella* ($p = 0.08$) compared to HIV−CAD− (Table 4). On the other hand, *Bacteroides* ($p = 0.0105$), *Butyricimonas* ($p = 0.04$), *Faecalibacterium* ($p < 0.00001$), *Flavonifractor* ($p = 0.02$), *Lachnospira* ($p < 0.00001$), *Lachnospira*_UCG-001 ($p < 0.00001$), *Lachnospira*_UCG-004 ($p < 0.001$), *Lachnospira*_NK4A136_group ($p = 0.03$), *Oscillibacter* ($p < 0.001$), and *Roseburia* ($p < 0.001$) were found to be significantly depleted in HIV+CAD+ compared to HIV−CAD+, and *Sutterella* ($p = 0.06$) followed the same trend without reaching statistical significance (Table 4). Another pattern of altered proportion of bacterial genera in the fecal microbiota of HIV+CAD+ participants was also observed, with a decrease in the abundance of several genera with HIV infection and with subclinical CAD. Indeed, compared to HIV−CAD−, HIV+CAD+ participants carried significantly less *Fusicatenibacter* ($p < 0.0001$), *Anaerosporobacter* ($p = 0.02$), *Erysipelotrichaceae*_UCG-003 ($p = 0.03$), *Romboutsia* ($p = 0.01$), and *Subdoligranulum* ($p = 0.01$) (Table 4). Fluctuations in some genera were also found to be driven by the presence of CAD within PWH and also in HIV− individuals. HIV+CAD+ individuals had a significantly lower abundance of *Fusicatenibacter* than HIV+CAD− ($p = 0.02$). In addition, HIV−CAD+ carried significantly less abundant *Blautia* than HIV−CAD− ($p = 0.03$). Moreover, HIV infection alone was also associated with a decrease in bacterial genera, with HIV+CAD− carrying significantly less abundant *Anaerosporobacter* ($p = 0.008$) and *Subdoligranulum* ($p = 0.02$) than HIV−CAD− (Table 4). Finally, two genera of the fecal microbiota showed a different pattern from the others, with a significant increase in abundance of *Alloprevotella* ($p = 0.01$) and *Catenisphaera* ($p = 0.02$) in HIV+CAD+ compared to HIV−CAD− (Table 4).

Correlations between plasma eCBome mediator levels, the composition of fecal microbiota, and clinical parameters of the study participants

To assess whether plasma levels of eCBs and their congeners were associated with clinical parameters related to HIV infection and CAD, correlation analyses were performed. Total cholesterol levels were positively associated with plasma levels of LEA in the whole study populations (Figures 2 and S2–S4), whereas in CAD+ and HIV+CAD+ individuals this parameter was also associated with SEA (Figures 2 and S4). Interestingly, when considering the whole study population, CAD+, or HIV+CAD+ status, triglyceride levels were positively associated with plasma levels of several MAGs, including 2-OG, 2-LG, 2-EPG, and 2-DPG (Figures 2, S2, and S4) along with 2-AG and 2-DHG in the HIV+ group (Figures S3). In HIV+CAD+ participants, plasma levels of several MAGs were associated with both duration of HIV infection and duration of ART, whereas plasma levels of NAEs PEA and DPA-EA(n-6) were negatively associated with these measures (Figure 2). Plasma levels of PEA were positively associated with two major clinical parameters of CAD, including the total plaque volume and the volume of low attenuation plaque, as well as the volume of fat near the right coronary artery, while being negatively correlated with epicardial fat attenuation (Figures 2 and S4). In HIV+CAD+ participants, 2-AG showed the inverse profile of what was observed for PEA for all these clinical measures (Figure 2). Like 2-AG, plasma levels of 2-DHG were also negatively associated with these major clinical parameters of CAD (Figure 2). Finally, among NAEs, only PEA levels were associated negatively with MAG levels, regardless of HIV or CAD status (Figures 2 and S2–S4).

Correlation analysis revealed unique interactions between the gut microbiota and the circulating eCBome depending on the analyzed study group (Figures 2 and S2–S4). In the whole study population, the family *Monoglobaceae* was negatively associated with SEA, OEA, 2-AG, and 2-DPG, whereas the families *Bacteroidaceae* and *Sutterellaceae* were negatively associated with 2-LG and 2-OG, with the former bacterial family positively associated with HbA1C levels and the latter one negatively associated with triglyceride levels (Figures S2). All these associations were lost within the HIV+ and CAD+ groups, except for the negative association between *Sutterellaceae* and 2-OG in HIV+ individuals (Figures S3 and S4). Importantly, in CAD+ only *Bacteroidaceae* was positively associated with PEA as well as right coronary artery fat volume, total plaque volume, and low attenuation plaque volume, while being negatively associated with epicardial fat attenuation (Figures S4). In HIV+CAD+ participants, *Bacteroidaceae* was also positively associated with total plaque volume and low-attenuation plaque volume (Figure 2). At the genus level, again in the whole study population, *Blautia* was positively associated with the NAEs, including AEA, LEA, OEA, and DHEA, whereas *Flavonifractor* was negatively associated with the 2-MAGs, including 2-AG, 2-DHG, 2-LG, and 2-OG as well as triglyceride and insulin levels (Figures S2). Again, no such associations were observed in the HIV+ and CAD+ groups, with *Blautia* instead being positively correlated with AEA levels in HIV+ (Figures 2, S3, and S4). *Bacteroides* was positively associated with total plaque volume and volume of low attenuation plaque, whereas *Catenisphaera* was negatively associated with these (Figures 2 and S4).

In contrast, within the HIV+ group, only the family *Marinifilaceae* was found to have significant negative associations with several NAEs (AEA, EPEA) and 2-MAGs (2-LG, 2-OG, and 2-EPG) (Figures S3). However, *Marinifilaceae* was negatively associated only with EPEA in HIV+CAD+ participants (Figure 2). At the genus level while *Butyricimonas* was similarly negatively associated with several 2-MAGs (2-LG, 2-OG, 2-DPG, and 2-DHG), all these associations were lost in HIV+CAD+ participants (Figures 2 and S3). In contrast, *CAG-56* was positively associated with several of the same 2-MAGs (2-OG, 2-EPG, 2-DPG) as well as triglycerides (Figures S3). Again, none of these associations were observed in the CAD+ and HIV+CAD+ groups (Figure 2). Instead, while in CAD+ participants, *Fusicatenibacter* was uniquely found to be negatively associated with the 2-MAGs, 2-LG, 2-OG, 2-EPG, 2-DPG, and triglyceride levels (Figures S4), all these associations were lost in HIV+ individuals (Figures 2 and S3). Finally, while *Bacteroides* correlated positively with total plaque volume and volume of low attenuation plaque, these CAD-related parameters correlated negatively with *Catenisphaera* (Figures 2 and S4).

DISCUSSION

The primary goal of this study was to determine whether the plasma levels of the two eCBs, AEA and 2-AG, and their NAE and 2-MAG congeners, respectively, were associated with subclinical CAD in PWH. We also assessed the association between this expanded eCB system, or

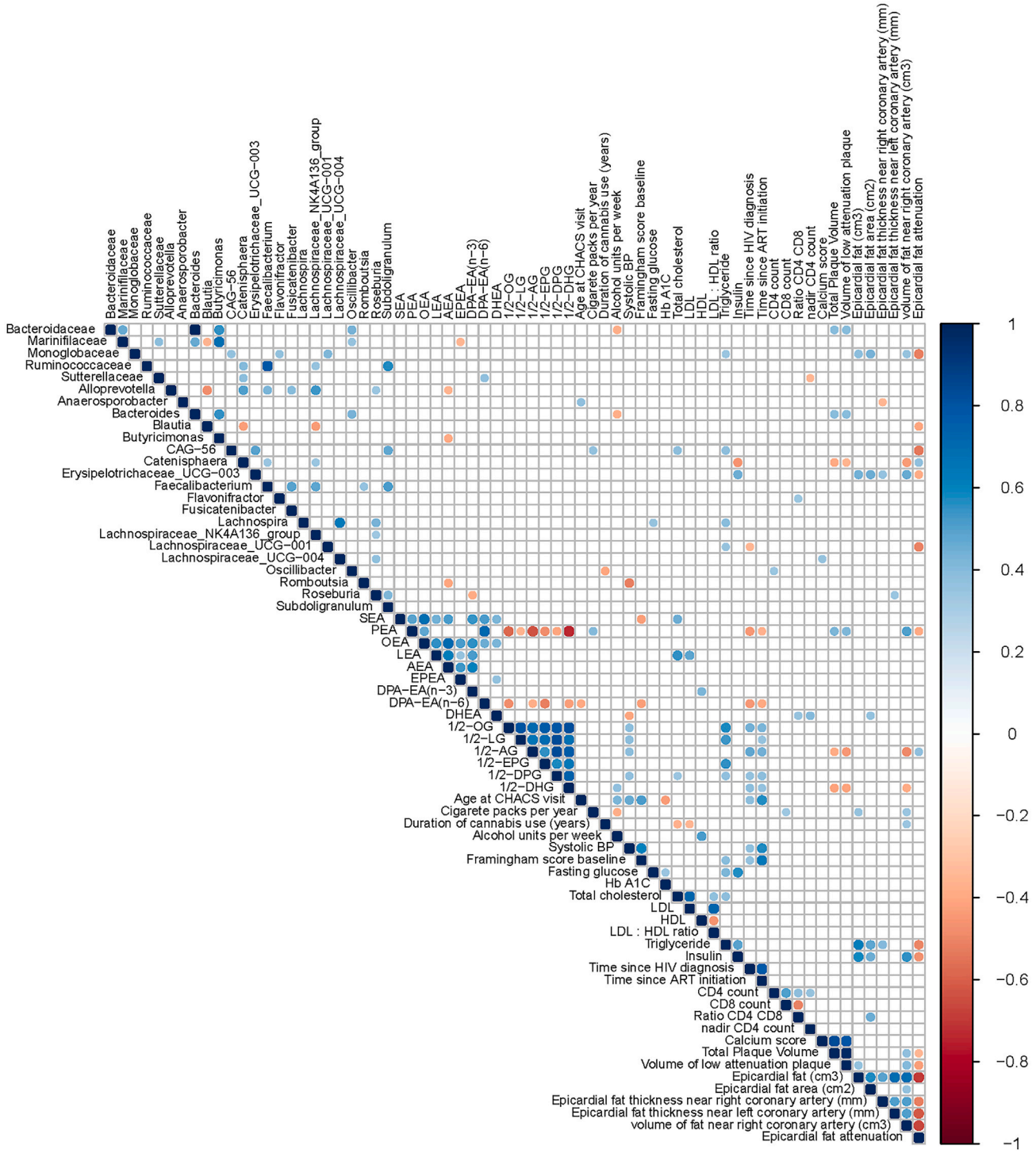

Figure 2. Heatmaps of Spearman correlations between plasma eCBome, fecal microbiota, clinical data, and risk factors associated to coronary artery disease (CAD) among HIV+CAD+ participants

Correlations are performed using the cor.test R function, with Bonferroni correction. Positive and negative correlations are displayed in blue and red, respectively, with color intensity being proportional to the coefficient's value. The ordinate axis on the right represents the scale of coefficients of the Spearman correlation. The two-abscissa axis represents plasma eCBome, fecal microbiota, clinical data, and risk factors associated with CAD. The significance level for *p* values was set at <0.05.

Nota bene: the correlations between microbial families and genus and other variables have been performed only on a subset of study participants from whom the stool specimens have been collected.

eCBome, and the gut microbiota in a subset of the study participants. Overall, we observed a peculiar pattern in plasma levels of eCBome mediators, with an inverse relationship between plasma NAE and MAG levels in PWH and HIV− individuals. Globally, PWH exhibited lower levels of AEA and its NAE congeners and higher levels of 2-AG and its MAG congeners. On the other hand, HIV− individuals displayed higher levels of AEA and several others NAEs and lower levels of several MAGs compared to PWH. When comparing the eCBome mediator plasma levels based on the CAD+ status, decreased levels of NAEs, EPEA and DHEA, and higher levels of only one MAG (2-OG) were observed compared to CAD− individuals. The similar inverse balance between NAEs and MAGs was also observed within PWH, with HIV+CAD+ individuals exhibiting lower levels of NAEs and higher levels of 2-OG compared to HIV+CAD− participants. Interestingly, PEA was the only eCBome mediator that showed a positive association with total atheroma plaque volume and low-attenuation plaque in individuals with subclinical CAD. In HIV+CAD+ individuals, this positive association with PEA and the two main subclinical CAD markers contrasted with the negative correlation between PEA and duration of HIV infection and duration of ART. A potential gut microbiota signature profile reflecting subclinical CAD was also characterized as shown by the positive association between *Bacteroidaceae* family and the *Bacteroides* genus (the likely driver for correlations observed for *Bacteroidaceae* to which it belongs), with both total atheroma and low-attenuation plaque volume. However, within HIV− individuals, no significant differences in the plasma levels of eCBome lipids were observed when comparing individuals with CAD and those without CAD. These findings, apart from confirming the different behavior of alterations in the circulating levels of NAEs and MAGs as documented in some previous human studies,[54–56] indicate for the first time that HIV infection and CAD are associated with similar alterations in eCBome mediators.

When comparing our finding of the absence of association between all other eCBome mediators and markers of subclinical CAD, with previous data showing that some NAEs or 2-MAGs are instead related to such markers in overweight individuals with overt CAD and without HIV[24,30,31,57], it is tempting to speculate that such changes are the consequence rather than the early cause (or marker) of clinical or acute CAD or of the transition into these conditions from subclinical CAD. Overall, these findings suggest that chronic HIV infection, but not subclinical CAD *per se*, significantly alters the circulating eCBome profile signature in PWH and that this alteration affects differentially the two main classes of eCBome mediators, NAEs and MAGs.

We found significantly lower plasma levels of AEA and several of its congeners including EPEA, LEA, DHEA, and DPA-EA(n-6) in PWH compared to HIV− control group. Our results are in line with the plasma profile of some NAEs depicted in a recent observational study, also showing lower concentrations of circulating AEA and OEA in PWH compared to HIV− controls.[53] These findings provide additional supportive evidence of the capacity of chronic HIV infection to significantly alter lipid metabolism globally[6,7] and particularly the class of lipids belonging to the eCBome, such as NAEs.[53] One possible way by which chronic HIV could lower the levels of AEA and other NAEs would be by disrupting the activity of the main enzymes involved in the metabolism of these lipids.[53] Indeed, the majority of NAEs, including AEA, are biosynthesized from the hydrolysis of cell membrane precursors, the *N*-acyl-phosphatidylethanolamines (NAPEs), mainly through the activity of NAPE-specific phospholipase D (NAPE-PLD).[15] In parallel, NAEs in humans are mainly hydrolyzed by two isoforms of fatty acid amide hydrolase (FAAH-1 and -2).[15] Thus, it could be envisioned that HIV could enhance degradation of NAEs by these enzymes and therefore reduce their circulating levels. Such a possibility has been validated in an animal model demonstrating that the HIV glycoprotein gp120 enhances the activity of FAAH, thus reducing the tissue concentrations of AEA.[58] Indeed, other studies have also shown increased levels of AEA after pharmacologic or genetic inhibition of FAAH.[11,59–61]

Another parameter to consider that could also affect plasma levels of NAEs in PWH is the use of lipid-lowering therapy such as statins. Indeed, given their elevated risk of developing CAD, PWH are very often prescribed statins, which have effectively demonstrated excellent efficacy in a large phase 3 randomized clinical trial by drastically reducing the risk of CAD development in PWH.[62] Indeed, statins reduce the levels of LDL cholesterol,[63] one of the main drivers of CAD. Therefore, a reduction in cholesterol-associated lipoproteins by statins could presumably also reduce the levels of certain NAEs. In our study, alongside with low levels of NAEs, PWH also exhibited low levels of LDL, HDL, and total cholesterol compared to HIV− controls. However, in our cohort, only around one-quarter of PWH were on statins when they were included in the study and no difference was observed in statin intake in HIV+ versus HIV− individuals. Further studies are nevertheless needed to better elucidate the relationship between NAEs and statin use in the context of HIV, as these molecules are strongly recommended for PWH as an efficient CAD preventive therapy.[62] Importantly, in a recent observational study involving PWH, Murray et al. showed that low levels of AEA and its congeners were accompanied by higher levels of soluble markers of systemic inflammation (TNFR2 and CD27).[53] As AEA and several of its NAE congeners are known to exert anti-inflammatory effects,[10–13,19,30] low circulating levels of these lipids in PWH could serve as an additional biomarker (and be one of the possible causes) of the chronic inflammatory status in PWH.

Unlike NAEs, we found significantly higher levels of several MAG congeners in PWH compared to HIV− controls. In contrast to our data, which show an increase of 2-AG levels and its congeners in PWH and its significant increase in HIV+CAD+ versus HIV−CAD+ individuals, Murray et al. did not find any significant impact of the HIV status on plasma levels of this eCB.[53] The large age difference between the two study cohorts may explain these discrepant observations. Indeed, elevated levels of 2-AG in plasma have been suggested as a biomarker of aging.[28] In the study by Murray et al., PWH were relatively young with a mean age of 32.5 years,[53] whereas in our study, PWH were on average 57.2 years old. Like AEA, 2-AG is described as having anti-inflammatory properties via activation of cannabinoid CB_2 receptors.[9,10,15,64,60] Therefore, since chronic HIV infection is associated with systemic inflammation,[6,7] one would also expect to observe a reduction in 2-AG levels in PWH compared to their HIV negative counterpart, as was the case for AEA and its NAE congeners. However, 2-AG has also been described to cause pro-inflammatory and atherogenic effects via activation of CB_1 receptors,[65,66] which would instead explain the higher levels of this compound in PWH. With regard to the higher levels of other MAGs, as in the case of NAEs, this could be explained by the fact that, within the same family of eCBome mediators, often the same enzymes regulate the biosynthesis and degradation

of different members of these families, and such enzymes could be disrupted in PWH. However, unlike NAEs, to the best of our knowledge, there is no previous evidence of MAG metabolic enzyme disruption in animal models of HIV infection.

At any rate, the inverse fluctuation of 2-AG compared to AEA in PWH supports the fact that chronic HIV disrupts lipid metabolism[6,7] and that this dysregulation affects differentially the metabolism of NAEs and MAGs such as 2-AG and AEA.[53] Indeed, while AEA is mainly biosynthesized by NAPE-PLD and hydrolyzed by FAAH,[15] one possible mechanism for the biosynthesis of plasma MAGs is through the sequential hydrolysis of triglycerides first and then diacylglycerols, for example in the visceral adipose tissue (VAT) or liver.[15] Accordingly, in our study, while within NAEs only plasma levels of LEA positively correlated with total cholesterol levels, several MAG congeners positively correlated with triglyceride levels. Importantly, in contrast to cholesterol, triglyceride levels were increased according to both HIV and CAD status, with the highest levels in HIV+CAD+ individuals among all study groups. Thus, dyslipidemia in PWH might alter MAGs and eventually contribute to preclinical CAD. Indeed, cross-sectional studies have shown elevated levels of 2-AG, but not AEA, in the VAT of obese people with elevated blood triglycerides.[25,26] Additionally, when obese individuals were submitted to a 1-year lifestyle change including healthy diet and physical activity, VAT and blood triglyceride reduction were correlated with a drastic decrease of 2-AG plasma levels, suggesting that a possible source of plasma 2-AG, and by extent its MAG congeners, are triglycerides coming from VAT.[25–27] Therefore, elevated levels of 2-AG and its congeners might be explained by the hypertriglyceridemia commonly observed in PWH taking ART.[67] Notably, duration of ART was associated with increased plasma levels of MAGs in HIV+CAD+ participants. The majority of PWH in our study were receiving nucleoside reverse-transcriptase inhibitor (NRTI) containing regimens for long periods, which might affect their blood triglyceride levels and, consequently, their 2-AG plasma levels. Indeed, hypertriglyceridemia is the most common type of dyslipidemia driven by certain antiretroviral molecules such as protease inhibitors as well as NRTIs and non-NRTIs that perturb lipid metabolism.[67] Although 2-AG and AEA levels were not significantly different between CAD+ and CAD− PWH, they followed the same pattern as their respective congeners. PWH with CAD had lower plasma levels of PEA, DHEA, and EPEA, which share the same metabolism as AEA,[15] while exhibiting higher plasma levels of 2-OG, a 2-AG congener.[15] Moreover, in PWH, DHEA inversely correlated with the increase in the number of cigarette packs smoked per year, a strong risk factor associated with CAD.[6,7] Interestingly, PEA, EPEA, and DHEA have been shown to exert anti-inflammatory properties,[12,16,18,68,69] and it has been suggested that dietary supplementation with these compounds or their fatty acid precursors may improve inflammatory conditions.[19] Importantly, within all eCBome mediators that we assessed, only PEA has been associated with clinical markers of CAD including total atheroma plaque volume and the low-attenuation plaque volume in CAD+ individuals. Indeed, PEA has been shown to be associated with worsened coronary function and arterial inflammation,[30] whereas its levels were shown to decrease with hypertension in elderly men,[29] possibly suggesting that enhancement or reduction of circulating PEA levels might represent an adaptive or maladaptive response to cardiometabolic risk. Indeed, PEA has been shown to promote attenuation of atherosclerotic plaque formation in mice[17] and of atherogenic inflammation.[66] On the other hand, although non-2-AG MAGs, such as 2-OG, are less studied, high levels of 2-AG have been shown to correlate positively with atherogenic markers, including hypertriglyceridemia in several pre-clinical studies,[20,21,27,28,31] supporting the hypotheses that (1) a major source of these MAG would be triglycerides (possibly deriving from the VAT), and (2) 2-AG, contrary to its role exerted when activating CB_2 receptors, exacerbates atherogenic inflammation by activating CB1 receptors.[65,66] Consistent with these hypotheses, we observed a strong positive correlation between 2-OG and other MAGs and triglyceride levels in individuals with CAD.

The gut microbiota has been shown to be widely altered both during CAD and following HIV infection[33–37,52] and to influence the eCBome system[35,47,70–73] While no major differences were observed in diversity among the four investigated study groups, three major patterns of alterations in bacterial families and/or genera were detected: (1) changes due to the presence of CAD observed only in the absence of HIV; (2) changes due to the presence of HIV only in individuals with CAD (i.e., significant when comparing the HIV+CAD+ with HIV−CAD+ group) or observed in the presence of both HIV and CAD (i.e., when comparing the HIV+CAD+ with the HIV−CAD− group), and (3) less frequently observed changes due to the presence of HIV only. The families *Marinifilaceae* and, possibly, *Sutterellaceae* ($p = 0.08$), which were increased by CAD and depleted by the concomitant presence of HIV, displayed pattern (1) above, whereas *Bacteroidaceae*, *Ruminococcaceae*, and *Monoglobaceae*, by being depleted by HIV but only in people with CAD, displayed pattern (2) above. Furthermore, the genera *Butyricimonas*, *Lachnospira*, *Lachnospira*_UCG-001, *Oscillibacter*, *Roseburia*, *Lachnospira*_UCG-004 ($p = 0.06$), and *Sutterella* ($p = 0.08$), by being increased by CAD in HIV− individuals and then decreased when HIV was present, showed pattern (1) above and so did *Blautia* by being decreased by CAD but only in the absence of HIV. On the other hand, the genera *Bacteroides*, *Faecalibacterium*, *Flavonifractor*, *Lachnospira*_NK4A136_group, and *Oscillibacter* were depleted in HIV+CAD+ compared to HIV−CAD+ and thus displayed pattern (2) above, as did *Fusicatenibacter*, *Erysipelotrichaceae*_UCG-003, and *Romboutsia*, which were depleted, and *Alloprevotella* and *Catenisphaera*, which were increased, in HIV+CAD+ compared to HIV−CAD− participants. Only the genera *Anaerosporobacter* and *Subdoligranulum*, by being decreased in HIV in the absence of CAD (and the former genus even more in the presence of CAD), display pattern (3) above.

These observations indicate that, in the CHACS cohort, subclinical CAD is a major determinant of fecal microbiota taxonomic alterations. However, the presence or absence of HIV also seems to drive some changes *per se* and, more frequently, plays a permissive role in the observed CAD-induced changes. Given the multifaceted role of most of the known species belonging to the altered genera, it is difficult to ascertain to what extent such alterations contribute to the various metabolic and inflammatory aspects of chronic HIV. In this sense, the observed correlation of some taxa with CAD and metabolic markers suggests a potential interplay between the changes in microbiota and eCBome mediators in the context of preclinical CAD. In particular, in the CAD+ cohort only, the *Bacteroidaceae* family and the *Bacteroides* genus were positively associated with PEA plasma levels. Regardless of HIV status, *Bacteroidaceae* and *Bacteroides* were associated with CAD major clinical markers, including total plaque volume and low attenuation plaque, while *Catenisphaera* were negatively associated

with them. The fact that PEA was the only eCBome mediator that was associated with CAD clinical markers, and PEA levels were exclusively enriched in HIV+CAD+ participants compared to HIV+CAD− participants, might suggest a potential signature of the interplay between the eCBome and gut dysbiosis in line with CAD development. Yet, the correlations between *Bacteroidaceae* and *Bacteroides* and PEA were only observed in the entire CAD+ and not HIV+CAD+ cohorts, perhaps because of the significantly smaller size of the latter. However, it cannot be ignored that both the *Bacteroidaceae* family and the *Bacteroides* genus were depleted in HIV+CAD+ versus HIV−CAD+, which raises a question on their functional link with the eCBome and CAD in PWH. Additionally, some of the fecal microbiota alterations may be suggestive also of changes in eCBome-based communication between host and gut bacteria in HIV+CAD+ individuals. As such, the reduction of *Bacteroides* in this group might possibly be driven by ART medication (although no correlation between these genera and the length of time of ART was observed). Furthermore, the reduction of *Bacteroides* in this group may also be suggestive of potentially reduced levels of non-NAE and non-MAG eCB-like molecules (which we did not measure in this study) produced by several species belonging to this genus.[74,75]

In sum, the observations that subclinical CAD, rather than chronic HIV and ART, drives most changes in the fecal microbiota composition, and that several of such changes are nevertheless reversed or unobserved with the cooccurrence of HIV, opens novel perspectives on the role of the gut microbiota in the partially overlapping inflammatory conditions accompanying subclinical CAD and HIV. The finding that no significant changes in circulating NAE and MAG levels were associated with subclinical CAD alone may suggest that eCBome mediators and gut microbiota composition are modulated by mostly non-overlapping mechanisms in our cohort.

In conclusion, chronic HIV infection profoundly alters the plasma level profile of eCBs and related mediators in PWH, marked by an inverse relationship between NAEs and MAGs. This signature pattern was almost maintained within HIV+CAD+ group, suggesting that chronic HIV infection, but not subclinical CAD, is the main driver of altered eCBome system in PWH. Regarding the gut microbiota taxonomic composition, this appeared to depend mostly on the presence of the subclinical CAD status, although the co-presence or absence of chronic HIV plays a permissive role in many of the observed alterations. Further studies are required to understand the main sources and mechanisms underlying the changes observed here in the circulating levels of eCBome mediators in the context of subclinical CAD in PWH and those interesting aletartions in gut microbiota composition observed in CAD that are "canceled" by a concurrent HIV status.

Limitations of the study

Our study has some limitations, in particular its cross-sectional design, which did not allow us to better elucidate the overtime relationship between changes in eCBome and development of subclinical CAD and to clearly explain the inverse plasma NAE and MAG profiles observed in PWH compared to their HIV− counterpart. A longitudinal follow-up of the participants with controlled diets and other parameters that influence lipid metabolism and the eCBome, such as statins, would be helpful to better understand the dynamic of these profiles in the context of HIV and CAD and their potentially causative or merely correlative role with these conditions. Another limitation of this study is the fact that our cohort, notably the PWH, is largely dominated by males, which might have biological impacts on the eCBome system and the gut microbiota. In addition, both current cannabis and tobacco smoking, as well as drug use, were higher in PWH versus HIV− controls, which might also affect eCBome mediators or gut microbiota composition. Likewise, tobacco smoking was also more common in CAD+ compared to CAD− participants, whereas cannabis use was more frequent in PWH. The non-uniform distribution of these consumption habits within the study groups could constitute a confounding factor. Indeed, the frequent use of these substances has been shown to affect eCBome mediators[76–78] and the composition of gut microbiota.[79,80] Moreover, in PWH, frequent tobacco smoking in combination of cannabis use has been shown to reverse the anti-inflammatory effects exerted by cannabis consumption alone.[81] The higher rates of CAD family history in CAD+ vs. CAD− participants in our study raises open questions about the potential impact of the genetic on eCBome in CAD pathogenesis. Finally, in this study we did not measure inflammatory markers to assess their association with the eCBome, which should be addressed in future studies.

STAR★METHODS

Detailed methods are provided in the online version of this paper and include the following:

- KEY RESOURCES TABLE
- RESOURCE AVAILABILITY
  - Lead contact
  - Materials availability
  - Data and code availability
- EXPERIMENTAL MODEL AND STUDY PARTICIPANT DETAILS
  - Study design and population
  - Ethics
  - Data collection and study procedures
- METHOD DETAILS
  - Blood sampling and processing
  - Quantification of the plasma levels of endocannabinoids and their congeners
  - Microbiota characterization
- QUANTIFICATION AND STATISTICAL ANALYSIS

SUPPLEMENTAL INFORMATION

Supplemental information can be found online at https://doi.org/10.1016/j.isci.2024.110456.

ACKNOWLEDGMENTS

The authors express their heartfelt gratitude to all the participants in this study for generously contributing their time and unwavering commitment. The authors also thank Elizabeth Dumais and Hilal Kalkan for their technical assistance.

Funding: this research was funded by Canadian Institutes of Health Research (CIHR) grant # 177334 to C.T.C., V.D., and M.A.J.; the Canadian HIV Trials Network (CTN PT043) to C.T.C., M.D., C.T., V.D., and M.A.J.; the Lotte & John Hecht Memorial Foundation to C.T.C.; and NIH (grant #R01AG054324) to C.T., M.D., and M.E. R.S.M.B. was supported by FRQS and CIHR postdoctoral fellowships. M.D. and C.T.C. are recipients of FRQ-S Junior 2 Chercheur Boursier Clinicien career award. C.T. colds the Pfizer Chair in Clinical and Translational Research on HIV. M.A.J. holds the tier 2 CIHR Canada Research Chair in Immuno-Virology. V.D. is Canada Excellence Research Chair on the Microbiome-Endocannabinoidome Axis in Metabolic Health, which is supported by the Canadian Federal Tri-Agency and the Canadian Fund for Innovation, Leaders Fund. G.G. is supported by the Joint International Research Unit on Chemical and Biochemical Studies on the Microbiome and its Impact on Metabolic Health and Nutrition (JIRU-MicroMeNu), which is supported by the Sentinelle Nord programme of Université Laval, in turn supported by the Canada First programme of the Canadian Federal Tri-Agency. The funders had no role in the design of this study; in the collection, analyses, or interpretation of data; in the writing of the manuscript; or in the decision to publish the results.

AUTHOR CONTRIBUTIONS

Conceptualization: C.T.C., V.D., and M.A.J.; data curation: R.S.M.B., G.G., C.M., N.N., Y.A., and M.M.P.; data analysis, interpretation, and validation: R.S.M.B., G.G., C.M., N.N., C.S., M.D., N.F., C.T.C., V.D., and M.A.J.; funding acquisition: C.T.C., V.D., and M.A.J.; methodology: M.D., C.S., N.F., V.D., and M.A.J.; project administration: M.M.P.; resources: M.D., C.T., M.E., C.C.L., M.M.P., S.M., and C.T.C.; supervision: V.D. and M.A.J.; validation: C.S., M.D., C.T.C., V.D., and M.A.J.; writing—original draft: R.S.M.B., C.S., V.D., and M.A.J. All authors contributed to the refinement of the study and reviewed, revised, and approved the final version of the manuscript.

DECLARATION OF INTERESTS

We have no competing interest to declare.

Received: February 14, 2024
Revised: May 7, 2024
Accepted: July 2, 2024
Published: July 5, 2024

REFERENCES

1. Maartens, G., Celum, C., and Lewin, S.R. (2014). HIV infection: epidemiology, pathogenesis, treatment, and prevention. Lancet *384*, 258–271. https://doi.org/10.1016/S0140-6736(14)60164-1.
2. Vachiat, A., McCutcheon, K., Tsabedze, N., Zachariah, D., and Manga, P. (2017). HIV and Ischemic Heart Disease. J. Am. Coll. Cardiol. *69*, 73–82. https://doi.org/10.1016/j.jacc.2016.09.979.
3. Kearns, A., Gordon, J., Burdo, T.H., and Qin, X. (2017). HIV-1-Associated Atherosclerosis: Unraveling the Missing Link. J. Am. Coll. Cardiol. *69*, 3084–3098. https://doi.org/10.1016/j.jacc.2017.05.012.
4. Shah, A.S.V., Stelzle, D., Lee, K.K., Beck, E.J., Alam, S., Clifford, S., Longenecker, C.T., Strachan, F., Bagchi, S., Whiteley, W., et al. (2018). Global Burden of Atherosclerotic Cardiovascular Disease in People Living With HIV: Systematic Review and Meta-Analysis. Circulation *138*, 1100–1112. https://doi.org/10.1161/CIRCULATIONAHA.117.033369.
5. Durand, M., Sheehy, O., Baril, J.G., Lelorier, J., and Tremblay, C.L. (2011). Association between HIV infection, antiretroviral therapy, and risk of acute myocardial infarction: a cohort and nested case-control study using Québec's public health insurance database. J. Acquir. Immune Defic. Syndr. *57*, 245–253. https://doi.org/10.1097/QAI.0b013e31821d33a5.
6. Henning, R.J., and Greene, J.N. (2023). The epidemiology, mechanisms, diagnosis and treatment of cardiovascular disease in adult patients with HIV. Am. J. Cardiovasc. Dis. *13*, 101–121.
7. Hsue, P.Y., and Waters, D.D. (2019). HIV infection and coronary heart disease: mechanisms and management. Nat. Rev. Cardiol. *16*, 745–759. https://doi.org/10.1038/s41569-019-0219-9.
8. Chu, L., Shu, Z., Gu, X., Wu, Y., Yang, J., and Deng, H. (2023). The Endocannabinoid System as a Potential Therapeutic Target for HIV-1-Associated Neurocognitive Disorder. Cannabis Cannabinoid Res. *8*, 445–463. https://doi.org/10.1089/can.2022.0267.
9. Montecucco, F., and Di Marzo, V. (2012). At the heart of the matter: the endocannabinoid system in cardiovascular function and dysfunction. Trends Pharmacol. Sci. *33*, 331–340. https://doi.org/10.1016/j.tips.2012.03.002.
10. Turcotte, C., Chouinard, F., Lefebvre, J.S., and Flamand, N. (2015). Regulation of inflammation by cannabinoids, the endocannabinoids 2-arachidonoyl-glycerol and arachidonoyl-ethanolamide, and their metabolites. J. Leukoc. Biol. *97*, 1049–1070. https://doi.org/10.1189/jlb.3RU0115-021R.
11. Mock, E.D., Gagestein, B., and van der Stelt, M. (2023). Anandamide and other N-acylethanolamines: A class of signaling lipids with therapeutic opportunities. Prog. Lipid Res. *89*, 101194. https://doi.org/10.1016/j.plipres.2022.101194.
12. Tyrtyshnaia, A., Konovalova, S., Bondar, A., Ermolenko, E., Sultanov, R., and Manzhulo, I. (2021). Anti-Inflammatory Activity of N-Docosahexaenoylethanolamine and N-Eicosapentaenoylethanolamine in a Mouse Model of Lipopolysaccharide-Induced Neuroinflammation. Int. J. Mol. Sci. *22*, 10728. https://doi.org/10.3390/ijms221910728.
13. Tyrtyshnaia, A.A., Egorova, E.L., Starinets, A.A., Ponomarenko, A.I., Ermolenko, E.V., and Manzhulo, I.V. (2020). N-Docosahexaenoylethanolamine Attenuates Neuroinflammation and Improves Hippocampal Neurogenesis in Rats with Sciatic Nerve Chronic Constriction Injury. Mar. Drugs *18*, 516. https://doi.org/10.3390/md18100516.
14. Turcotte, C., Blanchet, M.R., Laviolette, M., and Flamand, N. (2016). The CB(2) receptor and its role as a regulator of inflammation.

Cell. Mol. Life Sci. *73*, 4449–4470. https://doi.org/10.1007/s00018-016-2300-4.
15. Simard, M., Archambault, A.S., Lavoie, J.C., Dumais, É., Di Marzo, V., and Flamand, N. (2022). Biosynthesis and metabolism of endocannabinoids and their congeners from the monoacylglycerol and N-acyl-ethanolamine families. Biochem. Pharmacol. *205*, 115261. https://doi.org/10.1016/j.bcp.2022.115261.
16. Park, T., Chen, H., Kevala, K., Lee, J.W., and Kim, H.Y. (2016). N-Docosahexaenoylethanolamine ameliorates LPS-induced neuroinflammation via cAMP/PKA-dependent signaling. J. Neuroinflammation *13*, 284. https://doi.org/10.1186/s12974-016-0751-z.
17. Rinne, P., Guillamat-Prats, R., Rami, M., Bindila, L., Ring, L., Lyytikäinen, L.P., Raitoharju, E., Oksala, N., Lehtimäki, T., Weber, C., et al. (2018). Palmitoylethanolamide Promotes a Proresolving Macrophage Phenotype and Attenuates Atherosclerotic Plaque Formation. Arterioscler. Thromb. Vasc. Biol. *38*, 2562–2575. https://doi.org/10.1161/atvbaha.118.311185.
18. Tyrtyshnaia, A., Bondar, A., Konovalova, S., Sultanov, R., and Manzhulo, I. (2020). N-Docosahexanoylethanolamine Reduces Microglial Activation and Improves Hippocampal Plasticity in a Murine Model of Neuroinflammation. Int. J. Mol. Sci. *21*, 9703. https://doi.org/10.3390/ijms21249703.
19. Tyrtyshnaia, A., Konovalova, S., Ponomarenko, A., Egoraeva, A., and Manzhulo, I. (2022). Fatty Acid-Derived N-acylethanolamines Dietary Supplementation Attenuates Neuroinflammation and Cognitive Impairment in LPS Murine Model. Nutrients *14*, 3879. https://doi.org/10.3390/nu14183879.
20. Jehle, J., Schöne, B., Bagheri, S., Avraamidou, E., Danisch, M., Frank, I., Pfeifer, P., Bindila, L., Lutz, B., Lütjohann, D., et al. (2018). Elevated levels of 2-arachidonoylglycerol promote atherogenesis in ApoE-/- mice. PLoS One *13*, e0197751. https://doi.org/10.1371/journal.pone.0197751.
21. Avraamidou, E., Nöthel, M., Danisch, M., Bindila, L., Schmidt, S.V., Lutz, B., Nickenig, G., and Jehle, J. (2023). Myeloid But Not Endothelial Expression of the CB2 Receptor Promotes Atherogenesis in the Context of Elevated Levels of the Endocannabinoid 2-Arachidonoylglycerol. J. Cardiovasc. Transl. Res. *16*, 491–501. https://doi.org/10.1007/s12265-022-10323-z.
22. Jehle, J., Hoyer, F.F., Schöne, B., Pfeifer, P., Schild, K., Jenniches, I., Bindila, L., Lutz, B., Lütjohann, D., Zimmer, A., and Nickenig, G. (2016). Myeloid-Specific Deletion of Diacylglycerol Lipase α Inhibits Atherogenesis in ApoE-Deficient Mice. PLoS One *11*, e0146267. https://doi.org/10.1371/journal.pone.0146267.
23. Vujic, N., Schlager, S., Eichmann, T.O., Madreiter-Sokolowski, C.T., Goeritzer, M., Rainer, S., Schauer, S., Rosenberger, A., Woelfler, A., Doddapattar, P., et al. (2016). Monoglyceride lipase deficiency modulates endocannabinoid signaling and improves plaque stability in ApoE-knockout mice. Atherosclerosis *244*, 9–21. https://doi.org/10.1016/j.atherosclerosis.2015.10.109.
24. Quercioli, A., Pataky, Z., Vincenti, G., Makoundou, V., Di Marzo, V., Montecucco, F., Carballo, S., Thomas, A., Staub, C., Steffens, S., et al. (2011). Elevated endocannabinoid plasma levels are associated with coronary circulatory dysfunction in obesity. Eur. Heart J. *32*, 1369–1378. https://doi.org/10.1093/eurheartj/ehr029.
25. Blüher, M., Engeli, S., Klöting, N., Berndt, J., Fasshauer, M., Bátkai, S., Pacher, P., Schön, M.R., Jordan, J., and Stumvoll, M. (2006). Dysregulation of the peripheral and adipose tissue endocannabinoid system in human abdominal obesity. Diabetes *55*, 3053–3060. https://doi.org/10.2337/db06-0812.
26. Côté, M., Matias, I., Lemieux, I., Petrosino, S., Alméras, N., Després, J.P., and Di Marzo, V. (2007). Circulating endocannabinoid levels, abdominal adiposity and related cardiometabolic risk factors in obese men. Int. J. Obes. *31*, 692–699. https://doi.org/10.1038/sj.ijo.0803539.
27. Di Marzo, V., Côté, M., Matias, I., Lemieux, I., Arsenault, B.J., Cartier, A., Piscitelli, F., Petrosino, S., Alméras, N., and Després, J.P. (2009). Changes in plasma endocannabinoid levels in viscerally obese men following a 1 year lifestyle modification programme and waist circumference reduction: associations with changes in metabolic risk factors. Diabetologia *52*, 213–217. https://doi.org/10.1007/s00125-008-1178-6.
28. Fanelli, F., Mezzullo, M., Belluomo, I., Di Lallo, V.D., Baccini, M., Ibarra Gasparini, D., Casadio, E., Mastroroberto, M., Vicennati, V., Gambineri, A., et al. (2017). Plasma 2-arachidonoylglycerol is a biomarker of age and menopause related insulin resistance and dyslipidemia in lean but not in obese men and women. Mol. Metabol. *6*, 406–415. https://doi.org/10.1016/j.molmet.2017.03.005.
29. Fanelli, F., Mezzullo, M., Repaci, A., Belluomo, I., Ibarra Gasparini, D., Di Dalmazi, G., Mastroroberto, M., Vicennati, V., Gambineri, A., Morselli-Labate, A.M., et al. (2018). Profiling plasma N-Acylethanolamine levels and their ratios as a biomarker of obesity and dysmetabolism. Mol. Metabol. *14*, 82–94. https://doi.org/10.1016/j.molmet.2018.06.002.
30. Quercioli, A., Carbone, F., Bonaventura, A., Liberale, L., Pataky, Z., Thomas, A., Lenglet, S., Lauer, E., Golay, A., Dallegri, F., et al. (2017). Plasma palmitoylethanolamide (PEA) as a potential biomarker for impaired coronary function. Int. J. Cardiol. *231*, 1–5. https://doi.org/10.1016/j.ijcard.2016.12.023.
31. Quercioli, A., Montecucco, F., Pataky, Z., Thomas, A., Ambrosio, G., Staub, C., Di Marzo, V., Ratib, O., Mach, F., Golay, A., and Schindler, T.H. (2013). Improvement in coronary circulatory function in morbidly obese individuals after gastric bypass-induced weight loss: relation to alterations in endocannabinoids and adipocytokines. Eur. Heart J. *34*, 2063–2073. https://doi.org/10.1093/eurheartj/eht085.
32. Piscitelli, F., and Silvestri, C. (2019). Role of the Endocannabinoidome in Human and Mouse Atherosclerosis. Curr. Pharmaceut. Des. *25*, 3147–3164. https://doi.org/10.2174/1381612825666190826162735.
33. Karlsson, F.H., Fåk, F., Nookaew, I., Tremaroli, V., Fagerberg, B., Petranovic, D., Bäckhed, F., and Nielsen, J. (2012). Symptomatic atherosclerosis is associated with an altered gut metagenome. Nat. Commun. *3*, 1245. https://doi.org/10.1038/ncomms2266.
34. Jie, Z., Xia, H., Zhong, S.L., Feng, Q., Li, S., Liang, S., Zhong, H., Liu, Z., Gao, Y., Zhao, H., et al. (2017). The gut microbiome in atherosclerotic cardiovascular disease. Nat. Commun. *8*, 845. https://doi.org/10.1038/s41467-017-00900-1.
35. Iannotti, F.A., and Di Marzo, V. (2021). The gut microbiome, endocannabinoids and metabolic disorders. J. Endocrinol. *248*. R83-r97. https://doi.org/10.1530/joe-20-0444.
36. Guida, F., Turco, F., Iannotta, M., De Gregorio, D., Palumbo, I., Sarnelli, G., Furiano, A., Napolitano, F., Boccella, S., Luongo, L., et al. (2018). Antibiotic-induced microbiota perturbation causes gut endocannabinoidome changes, hippocampal neuroglial reorganization and depression in mice. Brain Behav. Immun. *67*, 230–245. https://doi.org/10.1016/j.bbi.2017.09.001.
37. Caesar, R., Fåk, F., and Bäckhed, F. (2010). Effects of gut microbiota on obesity and atherosclerosis via modulation of inflammation and lipid metabolism. J. Intern. Med. *268*, 320–328. https://doi.org/10.1111/j.1365-2796.2010.02270.x.
38. Masenga, S.K., Hamooya, B., Hangoma, J., Hayumbu, V., Ertuglu, L.A., Ishimwe, J., Rahman, S., Saleem, M., Laffer, C.L., Elijovich, F., and Kirabo, A. (2022). Recent advances in modulation of cardiovascular diseases by the gut microbiota. J. Hum. Hypertens. *36*, 952–959. https://doi.org/10.1038/s41371-022-00698-6.
39. Bin Waleed, K., Lu, Y., Liu, Q., Zeng, F., Tu, H., Wei, Y., Xu, S., Zhang, Z., Rongfeng, Y., Fan, A., et al. (2020). Association of trimethylamine N-oxide with coronary atherosclerotic burden in patients with non-ST-segment elevation myocardial infarction. Medicine (Baltim.) *99*, e20794. https://doi.org/10.1097/MD.0000000000020794.
40. Sheng, Z., Tan, Y., Liu, C., Zhou, P., Li, J., Zhou, J., Chen, R., Chen, Y., Song, L., Zhao, H., and Yan, H. (2019). Relation of Circulating Trimethylamine N-Oxide With Coronary Atherosclerotic Burden in Patients With ST-segment Elevation Myocardial Infarction. Am. J. Cardiol. *123*, 894–898. https://doi.org/10.1016/j.amjcard.2018.12.018.
41. Waleed, K.B., Tse, G., Lu, Y.K., Peng, C.N., Tu, H., Ding, L.G., Xia, Y.L., Wu, S.L., Li, X.T., Zhou, H.Q., et al. (2021). Trimethylamine N-oxide is associated with coronary atherosclerotic burden in non-ST-segment myocardial infarction patients: SZ-NSTEMI prospective cohort study. Rev. Cardiovasc. Med. *22*, 231–238. https://doi.org/10.31083/j.rcm.2021.01.299.
42. Lu, Y., Zhang, Y., Zhao, X., Shang, C., Xiang, M., Li, L., and Cui, X. (2022). Microbiota-derived short-chain fatty acids: Implications for cardiovascular and metabolic disease. Front. Cardiovasc. Med. *9*, 900381. https://doi.org/10.3389/fcvm.2022.900381.
43. Lu, Q., Chen, J., Jiang, L., Geng, T., Tian, S., Liao, Y., Yang, K., Zheng, Y., He, M., Tang, H., et al. (2024). Gut microbiota-derived secondary bile acids, bile acids receptor polymorphisms, and risk of cardiovascular disease in individuals with newly diagnosed type 2 diabetes: a cohort study. Am. J. Clin. Nutr. *119*, 324–332. https://doi.org/10.1016/j.ajcnut.2023.08.023.
44. Zhang, S., Zhou, J., Wu, W., Zhu, Y., and Liu, X. (2023). The Role of Bile Acids in Cardiovascular Diseases: from Mechanisms to Clinical Implications. Aging Dis. *14*, 261–282. https://doi.org/10.14336/AD.2022.0817.
45. Chong Nguyen, C., Duboc, D., Rainteau, D., Sokol, H., Humbert, L., Seksik, P., Bellino, A.,

Abdoul, H., Bouazza, N., Treluyer, J.M., et al. (2021). Circulating bile acids concentration is predictive of coronary artery disease in human. Sci. Rep. *11*, 22661. https://doi.org/10.1038/s41598-021-02144-y.

46. Fornelos, N., Franzosa, E.A., Bishai, J., Annand, J.W., Oka, A., Lloyd-Price, J., Arthur, T.D., Garner, A., Avila-Pacheco, J., Haiser, H.J., et al. (2020). Growth effects of N-acylethanolamines on gut bacteria reflect altered bacterial abundances in inflammatory bowel disease. Nat. Microbiol. *5*, 486–497. https://doi.org/10.1038/s41564-019-0655-7.
47. Cani, P.D., Plovier, H., Van Hul, M., Geurts, L., Delzenne, N.M., Druart, C., and Everard, A. (2016). Endocannabinoids–at the crossroads between the gut microbiota and host metabolism. Nat. Rev. Endocrinol. *12*, 133–143. https://doi.org/10.1038/nrendo.2015.211.
48. Cluny, N.L., Keenan, C.M., Reimer, R.A., Le Foll, B., and Sharkey, K.A. (2015). Prevention of Diet-Induced Obesity Effects on Body Weight and Gut Microbiota in Mice Treated Chronically with Δ9-Tetrahydrocannabinol. PLoS One *10*, e0144270. https://doi.org/10.1371/journal.pone.0144270.
49. Mehrpouya-Bahrami, P., Chitrala, K.N., Ganewatta, M.S., Tang, C., Murphy, E.A., Enos, R.T., Velazquez, K.T., McCellan, J., Nagarkatti, M., and Nagarkatti, P. (2017). Blockade of CB1 cannabinoid receptor alters gut microbiota and attenuates inflammation and diet-induced obesity. Sci. Rep. *7*, 15645. https://doi.org/10.1038/s41598-017-15154-6.
50. Dione, N., Lacroix, S., Taschler, U., Deschenes, T., Abolghasemi, A., Leblanc, N., Di Marzo, V., and Silvestri, C. (2020). Mgll Knockout Mouse Resistance to Diet-Induced Dysmetabolism Is Associated with Altered Gut Microbiota. Cells *9*, 2705. https://doi.org/10.3390/cells9122705.
51. Srivastava, R.K., Lutz, B., and Ruiz de Azua, I. (2022). The Microbiome and Gut Endocannabinoid System in the Regulation of Stress Responses and Metabolism. Front. Cell. Neurosci. *16*, 867267. https://doi.org/10.3389/fncel.2022.867267.
52. Neff, C.P., Krueger, O., Xiong, K., Arif, S., Nusbacher, N., Schneider, J.M., Cunningham, A.W., Armstrong, A., Li, S., McCarter, M.D., et al. (2018). Fecal Microbiota Composition Drives Immune Activation in HIV-infected Individuals. EBioMedicine *30*, 192–202. https://doi.org/10.1016/j.ebiom.2018.03.024.
53. Murray, C.H., Javanbakht, M., Cho, G.D., Gorbach, P.M., Fulcher, J.A., and Cooper, Z.D. (2024). Changes in Immune-Related Biomarkers and Endocannabinoids as a Function of Frequency of Cannabis Use in People Living With and Without HIV. Cannabis Cannabinoid Res. *9*, e897–e906. https://doi.org/10.1089/can.2022.0287.
54. Pavon, F.J., Araos, P., Pastor, A., Calado, M., Pedraz, M., Campos-Cloute, R., Ruiz, J.J., Serrano, A., Blanco, E., Rivera, P., et al. (2013). Evaluation of plasma-free endocannabinoids and their congeners in abstinent cocaine addicts seeking outpatient treatment: impact of psychiatric co-morbidity. Addiction Biol. *18*, 955–969. https://doi.org/10.1111/adb.12107.
55. Bashashati, M., Bradshaw, H.B., Johnson, C.T., Zuckerman, M.J., Sarosiek, J., McCallum, R.W., and Sarosiek, I. (2023). Plasma endocannabinoids and cannabimimetic fatty acid derivatives are altered in cyclic vomiting syndrome: The effects of sham feeding. J. Invest. Med. *71*, 821–829. https://doi.org/10.1177/10815589231196591.
56. van Eyk, H.J., van Schinkel, L.D., Kantae, V., Dronkers, C.E.A., Westenberg, J.J.M., de Roos, A., Lamb, H.J., Jukema, J.W., Harms, A.C., Hankemeier, T., et al. (2018). Caloric restriction lowers endocannabinoid tonus and improves cardiac function in type 2 diabetes. Nutr. Diabetes *8*, 6. https://doi.org/10.1038/s41387-017-0016-7.
57. Jehle, J., Goerich, H., Bindila, L., Lutz, B., Nickenig, G., and Tiyerili, V. (2019). Endocannabinoid 2-arachidonoylglycerol is elevated in the coronary circulation during acute coronary syndrome. PLoS One *14*, e0227142. https://doi.org/10.1371/journal.pone.0227142.
58. Maccarrone, M., Piccirilli, S., Battista, N., Del Duca, C., Nappi, G., Corasaniti, M.T., Finazzi-Agrò, A., and Bagetta, G. (2004). Enhanced anandamide degradation is associated with neuronal apoptosis induced by the HIV-1 coat glycoprotein gp120 in the rat neocortex. J. Neurochem. *89*, 1293–1300. https://doi.org/10.1111/j.1471-4159.2004.02430.x.
59. Alhouayek, M., Bottemanne, P., Makriyannis, A., and Muccioli, G.G. (2017). N-acylethanolamine-hydrolyzing acid amidase and fatty acid amide hydrolase inhibition differentially affect N-acylethanolamine levels and macrophage activation. Biochim. Biophys. Acta. Mol. Cell Biol. Lipids *1862*, 474–484. https://doi.org/10.1016/j.bbalip.2017.01.001.
60. Turcotte, C., Archambault, A.S., Dumais, É., Martin, C., Blanchet, M.R., Bissonnette, E., Ohashi, N., Yamamoto, K., Itoh, T., Laviolette, M., et al. (2020). Endocannabinoid hydrolysis inhibition unmasks that unsaturated fatty acids induce a robust biosynthesis of 2-arachidonoyl-glycerol and its congeners in human myeloid leukocytes. Faseb. J. *34*, 4253–4265. https://doi.org/10.1096/fj.201902916R.
61. Xie, X., Li, Y., Xu, S., Zhou, P., Yang, L., Xu, Y., Qiu, Y., Yang, Y., and Li, Y. (2021). Genetic Blockade of NAAA Cell-specifically Regulates Fatty Acid Ethanolamides (FAEs) Metabolism and Inflammatory Responses. Front. Pharmacol. *12*, 817603. https://doi.org/10.3389/fphar.2021.817603.
62. Grinspoon, S.K., Fitch, K.V., Zanni, M.V., Fichtenbaum, C.J., Umbleja, T., Aberg, J.A., Overton, E.T., Malvestutto, C.D., Bloomfield, G.S., Currier, J.S., et al. (2023). Pitavastatin to Prevent Cardiovascular Disease in HIV Infection. N. Engl. J. Med. *389*, 687–699. https://doi.org/10.1056/NEJMoa2304146.
63. Aberg, J.A., Sponseller, C.A., Ward, D.J., Kryzhanovski, V.A., Campbell, S.E., and Thompson, M.A. (2017). Pitavastatin versus pravastatin in adults with HIV-1 infection and dyslipidaemia (INTREPID): 12 week and 52 week results of a phase 4, multicentre, randomised, double-blind, superiority trial. Lancet. HIV *4*, e284–e294. https://doi.org/10.1016/s2352-3018(17)30075-9.
64. Montecucco, F., Di Marzo, V., da Silva, R.F., Vuilleumier, N., Capettini, L., Lenglet, S., Pagano, S., Piscitelli, F., Quintao, S., Bertolotto, M., et al. (2012). The activation of the cannabinoid receptor type 2 reduces neutrophilic protease-mediated vulnerability in atherosclerotic plaques. Eur. Heart J. *33*, 846–856. https://doi.org/10.1093/eurheartj/ehr449.
65. Mach, F., Montecucco, F., and Steffens, S. (2009). Effect of blockage of the endocannabinoid system by CB(1) antagonism on cardiovascular risk. Pharmacol. Rep. *61*, 13–21. https://doi.org/10.1016/s1734-1140(09)70003-9.
66. Montecucco, F., Matias, I., Lenglet, S., Petrosino, S., Burger, F., Pelli, G., Braunersreuther, V., Mach, F., Steffens, S., and Di Marzo, V. (2009). Regulation and possible role of endocannabinoids and related mediators in hypercholesterolemic mice with atherosclerosis. Atherosclerosis *205*, 433–441. https://doi.org/10.1016/j.atherosclerosis.2008.12.040.
67. Yu, X.D., Huang, H., Jiao, Y., Li, J., Fan, X., Zhang, D., and Wang, F.S. (2023). Incidence and risk factors of hypertriglyceridemia in males with human immunodeficiency virus who are treated with combination antiretroviral therapy: a retrospective cohort study. Lipids Health Dis. *22*, 27. https://doi.org/10.1186/s12944-023-01786-3.
68. Meijerink, J., Balvers, M., and Witkamp, R. (2013). N-Acyl amines of docosahexaenoic acid and other n-3 polyunsatured fatty acids - from fishy endocannabinoids to potential leads. Br. J. Pharmacol. *169*, 772–783. https://doi.org/10.1111/bph.12030.
69. de Bus, I., van Krimpen, S., Hooiveld, G.J., Boekschoten, M.V., Poland, M., Witkamp, R.F., Albada, B., and Balvers, M.G.J. (2021). Immunomodulating effects of 13- and 16-hydroxylated docosahexaenoyl ethanolamide in LPS stimulated RAW264.7 macrophages. Biochim. Biophys. Acta. Mol. Cell Biol. Lipids *1866*, 158908. https://doi.org/10.1016/j.bbalip.2021.158908.
70. Muccioli, G.G., Naslain, D., Bäckhed, F., Reigstad, C.S., Lambert, D.M., Delzenne, N.M., and Cani, P.D. (2010). The endocannabinoid system links gut microbiota to adipogenesis. Mol. Syst. Biol. *6*, 392. https://doi.org/10.1038/msb.2010.46.
71. Ortiz-Alvarez, L., Xu, H., Di, X., Kohler, I., Osuna-Prieto, F.J., Acosta, F.M., Vilchez-Vargas, R., Link, A., Plaza-Díaz, J., van der Stelt, M., et al. (2022). Plasma Levels of Endocannabinoids and Their Analogues Are Related to Specific Fecal Bacterial Genera in Young Adults: Role in Gut Barrier Integrity. Nutrients *14*, 2143. https://doi.org/10.3390/nu14102143.
72. Manca, C., Boubertakh, B., Leblanc, N., Deschenes, T., Lacroix, S., Martin, C., Houde, A., Veilleux, A., Flamand, N., Muccioli, G.G., et al. (2020). Germ-free mice exhibit profound gut microbiota-dependent alterations of intestinal endocannabinoidome signaling. J. Lipid Res. *61*, 70–85. https://doi.org/10.1194/jlr.RA119000424.
73. Silvestri, C., and Di Marzo, V. (2023). The Gut Microbiome-Endocannabinoidome Axis: A New Way of Controlling Metabolism, Inflammation, and Behavior. Function (Oxf) *4*, zqad003. https://doi.org/10.1093/function/zqad003.
74. Cohen, L.J., Kang, H.S., Chu, J., Huang, Y.H., Gordon, E.A., Reddy, B.V., Ternei, M.A., Craig, J.W., and Brady, S.F. (2015). Functional metagenomic discovery of bacterial effectors in the human microbiome and isolation of commendamide, a GPCR G2A/132 agonist. Proc. Natl. Acad. Sci. USA *112*, E4825–E4834. https://doi.org/10.1073/pnas.1508737112.
75. Lynch, A., Crowley, E., Casey, E., Cano, R., Shanahan, R., McGlacken, G., Marchesi, J.R., and Clarke, D.J. (2017). The Bacteroidales produce an N-acylated derivative of glycine with both cholesterol-solubilising and

hemolytic activity. Sci. Rep. *7*, 13270. https://doi.org/10.1038/s41598-017-13774-6.

76. Morgan, C.J., Page, E., Schaefer, C., Chatten, K., Manocha, A., Gulati, S., Curran, H.V., Brandner, B., and Leweke, F.M. (2013). Cerebrospinal fluid anandamide levels, cannabis use and psychotic-like symptoms. Br. J. Psychiatry *202*, 381–382. https://doi.org/10.1192/bjp.bp.112.121178.
77. Kearney-Ramos, T., Herrmann, E.S., Belluomo, I., Matias, I., Vallee, M., Monlezun, S., Piazza, P.V., and Haney, M. (2023). The Relationship Between Circulating Endogenous Cannabinoids and the Effects of Smoked Cannabis. Cannabis Cannabinoid Res. *8*, 1069–1078. https://doi.org/10.1089/can.2021.0185.
78. Centonze, D., Battista, N., Rossi, S., Mercuri, N.B., Finazzi-Agro, A., Bernardi, G., Calabresi, P., and Maccarrone, M. (2004). A critical interaction between dopamine D2 receptors and endocannabinoids mediates the effects of cocaine on striatal gabaergic Transmission. Neuropsychopharmacology *29*, 1488–1497. https://doi.org/10.1038/sj.npp.1300458.
79. Shapiro, H., Goldenberg, K., Ratiner, K., and Elinav, E. (2022). Smoking-induced microbial dysbiosis in health and disease. Clin. Sci. *136*, 1371–1387. https://doi.org/10.1042/CS20220175.
80. Liu, Y., Zhang, P., Sheng, H., Xu, D., Li, D., and An, L. (2023). 16S rRNA gene sequencing and machine learning reveal correlation between drug abuse and human host gut microbiota. Addiction Biol. *28*, e13311. https://doi.org/10.1111/adb.13311.
81. Yin, L., Dinasarapu, A.R., Borkar, S.A., Chang, K.F., De Paris, K., Kim-Chang, J.J., Sleasman, J.W., and Goodenow, M.M. (2022). Anti-inflammatory effects of recreational marijuana in virally suppressed youth with HIV-1 are reversed by use of tobacco products in combination with marijuana. Retrovirology *19*, 10. https://doi.org/10.1186/s12977-022-00594-4.
82. Durand, M., Chartrand-Lefebvre, C., Baril, J.G., Trottier, S., Trottier, B., Harris, M., Walmsley, S., Conway, B., Wong, A., Routy, J.P., et al. (2017). The Canadian HIV and aging cohort study - determinants of increased risk of cardio-vascular diseases in HIV-infected individuals: rationale and study protocol. BMC Infect. Dis. *17*, 611. https://doi.org/10.1186/s12879-017-2692-2.
83. Giguere, K., Chartrand-Lefebvre, C., Baril, J.G., Conway, B., El-Far, M., Falutz, J., Harris, M., Jenabian, M.A., Leipsic, J., Loutfy, M., et al. (2023). Baseline characteristics of a prospective cohort study of aging and cardiovascular diseases among people living with HIV. HIV Med. *24*, 1210–1221. https://doi.org/10.1111/hiv.13550.
84. Chen, Z., Boldeanu, I., Nepveu, S., Durand, M., Chin, A.S., Kauffmann, C., Mansour, S., Soulez, G., Tremblay, C., and Chartrand-Lefebvre, C. (2017). In vivo coronary artery plaque assessment with computed tomography angiography: is there an impact of iterative reconstruction on plaque volume and attenuation metrics? Acta Radiol. *58*, 660–669. https://doi.org/10.1177/0284185116664229.
85. Everard, A., Plovier, H., Rastelli, M., Van Hul, M., de Wouters d'Oplinter, A., Geurts, L., Druart, C., Robine, S., Delzenne, N.M., Muccioli, G.G., et al. (2019). Intestinal epithelial N-acylphosphatidylethanolamine phospholipase D links dietary fat to metabolic adaptations in obesity and steatosis. Nat. Commun. *10*, 457. https://doi.org/10.1038/s41467-018-08051-7.
86. Callahan, B.J., McMurdie, P.J., Rosen, M.J., Han, A.W., Johnson, A.J., and Holmes, S.P. (2016). DADA2: High-resolution sample inference from Illumina amplicon data. Nat. Methods *13*, 581–583. https://doi.org/10.1038/nmeth.3869.
87. McLaren, M.R., and Callahan, B.J. (2021). Silva 138.1 Prokaryotic SSU Taxonomic Training Data Formatted for DADA2 (Zenodo).
88. Anderson, M.J. (2017). Permutational Multivariate Analysis of Variance (PERMANOVA). In Wiley StatsRef: Statistics Reference Online, pp. 1–15. https://doi.org/10.1002/9781118445112.stat07841.

STAR★METHODS

KEY RESOURCES TABLE

REAGENT or RESOURCE	SOURCE	IDENTIFIER
Biological samples		
Human plasma	Biospecimens obtained from the Canadian HIV and aging cohort (CHACS, CTN 272) biobank, in compliance with the informed consent signed by participants	https://www.hivnet.ubc.ca/study/ctn-272-canadian-hiv-and-aging-cohort/
Human feces	Biospecimens obtained from the Canadian HIV and aging cohort (CHACS, CTN 272) biobank, in compliance with the informed consent signed by participants	https://www.hivnet.ubc.ca/study/ctn-272-canadian-hiv-and-aging-cohort/
Chemicals, peptides, and recombinant proteins		
Chloroform	Sigma	Cat# 650498
Methanol	Fisher	Cat# A4564
Water (LC-MS grade)	Fisher	Cat# w64
1-AG-D5	Cayman Chemical	Cat# 362152
AEA-d4	Cayman Chemical	Cat# 10011178
LEA-d4	Cayman Chemical	Cat# 9000553
DHEA-D4	Cayman Chemical	Cat# 9001108
AA-D8	Cayman Chemical	Cat# 390010
DHA-d5	Cayman Chemical	Cat# 10005057
Critical commercial assays		
DNeasy PowerSoil Pro Kit	QIAGEN	47016
Agencourt AMPure XP kit	Beckman Coulter Life Sciences	A63881
KAPA HiFi HotStart ReadyMix	Cedarlanes	KK2602
Miseq reagent v3 (600cycle)	Illlumina	MS-102-3003
PhiX Control v3	Illlumina	FC-110-3001
Nextera XT Index Kit V2 Set A (96 indexes, 384 samples)	Illumina	FC-131-2004
Nextera XT Index Kit V2 Set D (96 indexes, 384 samples)	Illumina	FC-131-2001
Oligonucleotides		
16S Amplicon PCR Forward Primer Ultramer 20 nmole TCGTCGGCAGCGTCAGATGTGTATA AGAGACAGCCTACGGGNGGCWGCAG	IDT	N.A.
16S Amplicon PCR Reverse Primer Ultramer 20 nmole GTCTCGTGGGCTCGGAGATGTGTAT AAGAGACAGGACTACHVGGGTATCTAATCC	IDT	N.A.
Software and algorithms		
GraphPad Prism Version 9.0	GraphPad	https://www.graphpad.com/
R Project	RStudio	https://posit.co/products/open-source/rstudio/

(*Continued on next page*)

Continued

REAGENT or RESOURCE	SOURCE	IDENTIFIER
DADA2 pipeline- microbiota	DADA2	https://benjjneb.github.io/dada2/tutorial.html
Other		
Clinical data related to HIV infection and CAD	Obtained from the Canadian HIV and aging cohort (CHACS, CTN 272)	https://www.hivnet.ubc.ca/study/ctn-272-canadian-hiv-and-aging-cohort/

RESOURCE AVAILABILITY

Lead contact

Further information and requests for resources and regents should be directed to and will be fulfilled by the lead contact, MA Jenabian: Jenabian.mohammad-ali@uqam.ca.

Materials availability

This study did not generate new unique reagents.

Data and code availability

- All data reported in this paper will be shared by the lead contact upon reasonable request.
- This paper does not report additional code.
- Any additional information required to reanalyze the data reported in this work paper is available from the lead contact upon reasonable request.

EXPERIMENTAL MODEL AND STUDY PARTICIPANT DETAILS

Study design and population

This study was an observational cross-sectional analysis among adult PWH recruited from the multicenter Canadian HIV and Aging Cohort (CHACS). The detailed information on the recruiting process and the cohort baseline characteristics has been published previously.[82,83] The main inclusion criteria were having a confirmed HIV infection lasting at least 15 years at the time of enrolment, being 40 years and older and being able to provide informed consent to participate to the study. In addition, an HIV-seronegative control group was also included from the CHACS cohort. Participant's biological sex, sexual orientation and ethnicity are described in Table 1. Participants were free of diagnosed cardiovascular disease (had never suffered a myocardial infarction, coronary revascularization, angina, stroke of peripheral vascular revascularization) prior to their enrolment in the study cohort. Coronary atherosclerotic plaque analysis was performed using contrast-enhanced coronary CT angiography images in all participants enrolled in the study cohort at the Centre Hospitalier de l'Université de Montréal, QC, Canada, and interpreted by a board-certified cardiothoracic radiologist (CCL).[84] All radiology personnel performing image interpretation and post-processing were blinded to HIV status.

Ethics

This study was approved by the research ethics board of the Centre Hospitalier de l'Université de Montréal (CHUM) (CE 11.063), MUHC: MP-37-2022-8107 and UQAM: 2022-4663 and conducted in conformity with the Declaration of Helsinki. All participants signed the written informed consent form of the study prior to enrollment.

Data collection and study procedures

At enrolment, participants completed study questionnaires, and underwent complete medical history and physical examination by a physician, participants data on vital signs, height, weight, and waist circumference were recorded, and routine laboratory blood tests and an electrocardiogram were performed. In addition, participants data were collected on sociodemographic factors, all past and current medication, medical conditions, including high blood pressure, diabetes, dyslipidemia, family history of premature CAD, risk factors for HIV transmission, and lifestyle habits (smoking, alcohol consumption, illicit drug use and level of physical activity). For participants with HIV, date of diagnosis and presumed mode of transmission was also recorded. In all participant enrolled in the study cohort, the presence of CAD was defined as total coronary plaque volume, measured on injected cardiac computed tomography (CT) scan.[82]

METHOD DETAILS

Blood sampling and processing

At enrolment, fasting blood was collected by venipuncture to measure circulating soluble markers including eCBs. Plasma was isolated via centrifugation and stored at –80°C to be analyzed in one batch at the end of the study enrolment. Participants also provided a specimen of stool which was immediately aliquoted and stored at –80°C until their batch analysis.

Quantification of the plasma levels of endocannabinoids and their congeners

For the quantification of MAGs, NAEs and fatty acids in human plasma, samples were processed and analyzed as documented by our team[60] with slight modifications. 200 μL of plasma samples were mixed with 300 μL of TRIS (pH 7.4, 50 mM). Toluene (2 ml) containing 0.1% acetic acid and the deuterated internal standards was then added to the samples, vortexed for 1 minute, centrifuged at 4000*g* for 5 minutes without brakes. Samples were next put in an ethanol-dry-ice bath (−80°C) to freeze the aqueous phase (bottom). The organic phase (top) was collected and evaporated to dryness under a stream of nitrogen. Samples were reconstituted in 30 μl of HPLC solvent A (H_2O with 0.05% acetic acid and 1 mM NH_4^+) and 30 μl of solvent B (MeCN/H_2O, 95/5, v/v, with 0.05% acetic acid and 1 mM NH_4^+). A 40 μl aliquot was injected onto an RP-HPLC column (Kinetex C8, 150 × 2.1 mm, 2.6 μm, Phenomenex). Quantification was performed on a Shimadzu 8050 triple quadrupole mass spectrometer using the same LC program as described previously.[85] Quantification was achieved by generating calibration curves using pure standards and analyzed on the LC-MS/MS system three times. The slope was then calculated using the ratio between the peak areas of the compound and its standard. For the MAGs, the data are presented as 2-MAGs but represent the combined signals from the *sn*-2- and -1(3) isomers as the latter are most likely generated from acyl migration from the *sn*-2 to the *sn*-1(3) position.

Microbiota characterization

DNA was extracted from feces using the QIAmp PowerFecal DNA kit (Qiagen, Hilden, Germany) according to the manufacturers' instructions. The DNA concentrations of the extracts were measured fluorometrically with the Quant-iT PicoGreen dsDNA Kit (Thermo Fisher Scientific, MA, USA) and the DNAs were stored at −20°C until sequencing library preparation. Sequencing libraries were produced according to the Illumina 16S ribosomal RNA gene V3-V4 region amplicon preparation protocol for the Illumina MiSeq System (primer pairs F (5′-TCGTCGGCAGCGTCAGATGTGTATAAGAGACAGCCTACGGGNGGCWGCAG- 3′) and, R (5′- GTCTCGTGGGCTCGGAGATGTGTATAAGAGACAGGACTACHVGGGTATCTAATCC- 3′) in conjunction with the QIAseq16S/ITS 384-Index I (Sets A, B, C, D) kit (Qiagen, Hilden, Germany). The 16S metagenomic libraries were eluted in 30 μl of nuclease-free water and 1μl was qualified with a Bioanalyser DNA 1000 Chip (Agilent, CA, USA) to verify the amplicon size (expected size ∼600 bp) and quantified with a Qubit (Thermo Fisher Scientific, MA, USA). Libraries were then normalized and pooled to 2nM, denatured and diluted to a final concentration of 6pM. Sequencing (2 × 300 bp paired-end) was performed using the MiSeq Reagent KitV3 (600 cycles) on an Illumina MiSeq System. Sequencing reads were generated in less than 65h. Image analysis and base calling were carried out directly on the MiSeq. Data was processed using the DADA2 pipeline according to the recommended workflow [86] and ASV sequences were assigned taxonomy using the most recent SILVA taxonomic database (SILVA SSURef 138.1 NR, March 2021) as a reference dataset using default parameters.[87] To deal with differences in sampling depth, the data rarefied to a depth of 10000 reads and rescaled to proportions for further analysis. Microbiota composition was assessed by calculating alpha and beta-diversity indexes obtained using the Phyloseq R package, and intra- and inter-individual variations in microbial composition using PERMANOVA (vegan R package).[88] Differential abundance testing of individual taxa was performed using two-way analysis of variance (ANOVA) followed by Tukey's multiple comparisons of means post-hoc test to generate p-values. All 16S sequencing data has been deposited in the NCBI with SRA accession number.

QUANTIFICATION AND STATISTICAL ANALYSIS

Descriptive statistics of quantitative variables were presented as median with interquartile range (IQR) and count data as frequency in percentage. Mann-Whitney *U* test was used to compare quantitative measurement between groups. Kruskal-Wallis rank sum test was used to compare more than two groups. GraphPad Prism Software (version 9.0.0, San Diego, CA, USA) was used for statistical analyses. Spearman test was used for correlations using the cor.test R function, with Bonferroni correction applied for multiple comparisons. The resulting correlation coefficients were represented in heatmaps, and the significance level for p-values was set at <0.05.